U.PORTO

Universidade do Porto
FEUP Faculdade de Engenharia

Development of a solution for the glass window breakage of MIC 7000

Ana Sofia Silveira Ribeiro

Dissertation submitted to
Faculdade de Engenharia da Universidade do Porto
for the degree of:

Master of Science in Mechanical Engineering

Supervisors
FEUP: Prof. Mário Vaz
Bosch: Eng. Pedro Bastardo

Porto, June 2017

Resumo

Esta dissertação foi realizada no âmbito do meu projeto de tese integrado num estágio curricular na Bosch Security Systems S.A. com o objetivo de propor soluções para um problema existente na linha de produção de um produto da empresa. O MIC 7000 é uma câmara de vigilância produzida pela unidade de Sistemas de Segurança da Bosch localizada em Ovar que recorrentemente tem sido alvo de rejeição devido à quebra da janela de vidro.

Após uma investigação interna que levou principalmente à análise dos componentes e das suas tolerâncias, mas sem sucesso, a Bosch contratou o INEGI com o objetivo de encontrar a causa raiz para o problema. Este projeto surge como resposta ao trabalho do INEGI no sentido de, analisando cada um dos fatores que contribui para a causa raiz, desenvolver um conjunto de soluções que eliminem ou minimizem o problema. De modo a ser possível compreender os conceitos que estão por detrás dos mecanismos de falha do(s) componente(s) e dos seus processos de fabrico, começou-se por fazer um estudo relativo à ciência do vidro, mecânica da fratura e fundição em alumínio.

De seguida, foi feita a descrição do problema, desde a caracterização dos componentes intervenientes, passando pela sua montagem na linha e pela análise às 2 investigações feitas no âmbito deste assunto, finalizando num estudo ao nível microscópico da superfície do vidro, que veio a confirmar suspeitas relativamente ao processo de endurecimento da janela.

Relativamente ao objetivo principal do projeto, as propostas de solução passaram pela substituição do tipo de vidro, quer por outro vidro mais resistente e apropriado ao endurecimento químico em causa, quer por um polímero. Além disso, 2 novas geometrias foram propostas de modo a eliminar os cantos, que implicam o aparecimento de zonas de concentração de tensões, e posteriormente foram simuladas tendo por base os elementos finitos, de modo a concluir se a sua implementação viria a prevenir a quebra da janela de vidro.

Por fim, as conclusões são relativas a todas as melhorias que poderão ser realizadas de modo a evitar a continuação do problema, passando não só pelas sugestões desenvolvidas neste projeto, mas também pelos pormenores que deverão ser considerados ao nível do rigor da produção dos componentes, introdução de tolerâncias mais precisas e do manuseamento das peças e limpeza das áreas de trabalho na linha de produção.

Palavras chave: Vidro, Concentração de Tensões, Elementos Finitos, Endurecimento Químico

Abstract

This dissertation was carried out within the scope of my master's thesis project integrated in a curricular internship at Bosch Security Systems S.A. with the main goal of proposing solutions to an existing problem in the production line of a company product. MIC 7000 is a surveillance camera produced by the Bosch Security Systems unit located in Ovar which has repeatedly been rejected due to glass window breaking.

After an internal investigation which led mainly to the analysis of the components and their tolerances, but without success, Bosch hired INEGI to find the root cause for the problem. This project comes as a response to the work carried out by INEGI in order to, by analyzing each of the factors that contribute to the root cause, develop a set of solutions that eliminate or minimize the problem. In order to be able to understand the concepts that lie behind the failure mechanisms of the component(s) and their manufacturing processes, a study on the science of glass was accomplished, as well as on fracture mechanics and casting in aluminum.

Afterwards, a description of the problem was made, including the characterization of the intervening components, the assembly in the line and the analysis of the 2 investigations made in this scope, finishing in a study at the microscopic level of the surface of the glass, which confirmed a suspicion related to the window strengthening process.

With regard to the main goal of this master's thesis, the proposed solutions include the replacement of the type of glass, either by another glass which is more resistant and appropriate to the chemical strengthening in question, or by a polymer. In addition, 2 new geometries were developed in order to eliminate the corners, which imply the appearance of stress concentration areas, and were later simulated on the basis of finite elements, so it would be possible to conclude if their implementation would prevent the glass window breakage.

Finally, the conclusions are related to all the improvements which can be made in order to avoid the continuation of the problem, not only regarding the suggestions developed throughout this project but also concerning the details that should be considered in terms of the rigor of the production of the components, introduction of more precise tolerances and of the handling of the parts and cleaning of the workstations in the production line.

Keywords: Glass, Stress Concentration, Finite Elements, Chemical Strenghening

Aos meus pais

Agradecimentos

Ao meu orientador Prof. Mário Vaz pela disponibilidade sempre demonstrada, pelos conselhos e pelo empenho. Ao Eng. Nuno Viriato, ao Prof. Paulo Tavares e ao Prof. Jaime Monteiro pelo apoio prestado ao longo deste projeto.

Ao Eng. Pedro Bastardo pela disponibilidade em me acolher e pela forma como me orientou em cada tarefa. Aos colegas do ENI que me ajudaram durante este projeto e com quem pude sempre aprender.

Ao prof. Paulo Tavares de Castro e Prof. Torres Marques pelo esclarecimento de dúvidas durante a realização da tese.

À minha família e aos meus amigos pelo apoio constante e por me acompanharem sempre.

List of symbols

T_g	Glass Temperature Transition
σ	Stress
E	Young's Modulus
ε	Strain
ν	Poisson's ratio
τ	Shear Stress
G	Shear Modulus
γ^*	Shear Strain
F	Force
σ_m	Theoretical Strength
γ	Fracture Surface Energy
r_0	Equilibrum space distance between atoms
σ_f	Pratical Strength
c*	Critical crack length
K_{IC}	Toughness
K_I	Stress Intensity factor
K_T	Stress Concentration factor
σ_i	Unform applied stress
α	Geometry correction factor
a	Crack length
D	Notch depth
ρ	Notch root radius
G	Energy release rate

Contents

List of Figures

List of Tables

Chapter 1

General Introduction

MIC7000 is a camera suitable for outdoor, industrial or commercial surveillance and which was introduced on the market in 2014 by Bosch Security Systems, in Ovar, and since then there has been a problem regarding the glass window. This component has been breaking during the production process and although Bosch has already tried to find the root cause, there have been no conclusions in response to this issue. Thus, the company hired INEGI (Institute of Science and Innovation in Mechanical and Industrial Engineering) in order to analyze the components and intervenient factors present in the production of this product which could lead to the breakage of the glass. This dissertation results from the analysis of the work carried out by INEGI in order to suggest solutions capable of solving the problem.

A brief introduction to Bosch was attained so the values of this company could be understood since this project resulted from an investigation work which took place in the Engineering Network Department of Bosch Security Systems in Ovar, for 5 months, and therefore, the vision and mission statement of the company was one of the main aspects to be considered during the internship.

The first approach to the issue involves an investigation considering the material in study – glass – including not only its characterization, but also the formation process and mechanical properties. Glass is an amorphous material, which implies the absence of a crystal network involving the absence of plasticity and therefore glass can only deform elastically or it will break [1]. This material is obtained by melting its components ensuring there is no crystallization, since the cooling rate is superior to the crystals formation rate and consequently a super cooled liquid is attained, leading to the formation of a short range periodic atomic arrangement.

Glass usually breaks due to a surface flaw where tension exceeds the practical strength of the glass. There is a significant difference between the theoretical and the pratical strength of glass and therefore, there have been several advances leading to decrease this difference and improve the latter, such as the build up of a residual compressive stress layer, up to a certain depth below the surface [2]. The most effective way to accomplish it is to immerse the glass in a molten alkali salt bath below the transition temperature. Regarding a soda lime silica glass, a potassium nitrate molten salt is recommended, since the basic principle is to exchange ions present in the glass for larger ones provided by the salt, resulting in surface stuffing of ions, and consequently on compression [3]. The performance of a chemically strengthened glass depends on the magnitude of the layer of compressive stress resultant from the ion exchange, as well as on the *case depth*, the thickness of this layer. However, the immersion of glass in a molten salt can also lead to relaxation of the surface compression which could be avoided by immersing it only for a

few minutes but on the other hand, the development of a larger case depth requires hours or even days [3].

An investigation on fracture mechanics was also carried out so the glass failure mechanism could be analyzed as well as the failure criteria and the surface markings. The fracture process which involves the formation of cracks depends on the microstructure of the amorphous solid, in this case, on the applied loading and on the environment. The precipitates, inclusions and grain size are features which act as imperfections and as the nuclei of the fracture[4].

The aluminum die casting process was described since 2 of the components are obtained through this process.

Moreover, the description of the problem includes a characterization of the different components, concerning the materials and relevant mechanical properties, such as density, yield strength and Poisson's ratio. The assembly in the production line was described step by step in order to analyze the factors which can possibly contribute to the glass window breakage. An internal report carried out by the processes department and the report provided by INEGI were considered when the solutions were developed, since both provide information regarding mainly the tolerances of the components, the analysis of particles present in some surfaces, the replacement of the gasket by another more rigid as a possiblity and the measurement of the deformation of the front shell and the glass window based on the ESPI method.

The solutions include the replacement of the glass for another type of glass, since an alkali-aluminasilicate glass is more appropriate for a chemical strengthening, stronger and would involve a deeper layer of compressive stress after strengthening. Another possibility is the replacement for a polymer, either a polycarbonate or an acrylic, and a comparison between both was accomplished, concluding an acrylic presents higher scratch resistance while a polycarbonate is significatly more resistant to impact. Besides, the glass geometry suffered some changes regarding the presence of the corners since a circular shape and a shape with rounded corners was simulated based on the finite elements method in order to be able to conclude if these modifications would eliminate the problem and prevent the breakage.

1.1 Motivation and Objectives

The main goal of this master's thesis is to start from the analysis of the report provided by INEGI and then develop a final solution to the problem regarding all the root causes where several factors were taken into account. In order to accomplish this goal it was necessary to use FEM analysis, deformation analysis techniques so everything is set to develop and test the proposed solutions and conclude if they would suit the company needs.

1.2 Bosch

It has always been an unbearable thought to me that someone could inspect one of my products and find it inferior in any way. For that reason I have constantly striven to produce products which withstand the closest scrutiny – products which prove themselves superior in every respect. Robert Bosch, 1918

Bosch started as a "Workshop for Precision Mechanics and Electrical Engineering" in 1886 created by Robert Bosch in Stuttgart alongside with a mechanic and an errand boy and nowadays is a global supplier of technology and services around the world divided

into three business sectors: Mobility Solutions, Consumer Goods and Energy and Building Technology, presented in figure 1.1, employing more than 300 000 people[5].

Figure 1.1: Bosch's services: Mobility Solutions, Consumer Goods and Energy and Building Techonology [5]

This group is made up of more than 440 subsidiaries and regional companies in about 60 countries, with 118 engineering locations worldwide. In addition, it is a company that gives a big importance to research and development and has the main objective of improving the quality of life of its customers by providing innovative and advantageous solutions. Besides the Bosch brand, this group offers other brands tailored to individual customer requirements that can also enhance the daily life [5].

Figure 1.2: Bosch around the world [5]

Robert Bosch GmbH has a special ownership structure that guarantees the business autonomy of the Bosch Group, making it possible for the company to plan over the long term and to make significant initial investments that ensures its future. 92 percent of the share capital of Robert Bosch GmbH is owned by Robert Bosch Stiftung GmbH, a nonprofit foundation while most of the voting rights are held by Robert Bosch Industrietreuhand KG, an industrial fiduciary society. Because of their business areas, Bosch can ensure the financing of their initiatives and the Robert Bosch Stiftung. The remaining shares are held by the Bosch family and Robert Bosch GmbH, as it is presented in figure 1.3 [5].

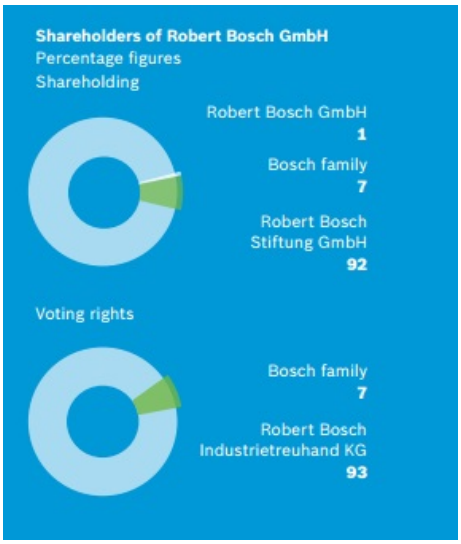

Figure 1.3: Shareholders of Robert Bosch GmbH [5]

1.2.1 Strategy

Bosch develops technology "invented for life", which means products that improve its clients's quality of life and help to preserve the natural resources which led Bosch to shape its changes according to the future and investing on fields related to connectivity, electrification, energetic efficiency, automation and emerging markets. Bosch also trusts and invests on their Investigation and Development team composed by 45 700 collaborators worldwide since its main aim is to motivate continuously their employees in order to develop their performance through more than 100 different schedules, international mobility programs and workshops opportunities during their professional path [5].

1.2.2 Bosch in Portugal

In Portugal, Bosch is represented in 4 different subsidiaries: Bosch Car Multimedia in Braga, Bosch Security Systems in Ovar, Bosch Thermotechnology in Aveiro and Robert Bosch in Lisbon. The Car Multimedia division focuses on smart solutions with the ability to make the vehicle integration of entertainment, navigation, telematics and driver assistance more flexible and more efficient. Bosch Security Systems is a global supplier of security, safety and communication products, services and solutions. Bosch Thermotechnology is an international manufacturer of water heaters and heating products. Bosch in Lisbon works as a sales office [5]. Robert Bosch was established in Portugal in 1911 being one of the top ten exporters in the country and is also one of the largest industrial employers with around 3 800 employees.

1.2.3 Bosch Security Systems Ovar

This business unit was founded in 1980 as a Philips 'subsidiary and later Bosch acquired it so it became a Bosch Security Systems unit (Bosch ST). Its headquarter is located in Ottobrunn, Germany while the continental distribution centers are Greer (USA), Straubing (Germany) and Taiwan. ST divisions are located in Hermosillo (Mexico), Lincoln (USA), Ovar (Portugal) and Zuhai (China). Bosch Ovar is located in the Industrial area of Ovar city, 30 km south from Oporto and works as an Electronics Manufacturing Service provider being part of Bosch Security Systems Division (ST).

Figure 1.4: Bosch ST fields [5]

It manufactures products for Business Unit Video Systems, Communication Systems, Fire and also products for other divisions, such as Thermotechnology:

- Video surveillance systems, IP video, video intelligent analysis, video for use in extreme conditions;
- Intrusion alarm systems
- Controlled access systems;
- Fire detection systems;
- Voice evacuation and communication systems;
- Management systems;
- Professional audio systems;
- Conference systems;
- Electronic components for other business units.

(a) Video system products (b) Communication products

Figure 1.5: Products from Bosch Ovar [5]

1.2.4 Departments

Each department reports to the plant manager António Pereira:

- MAT – Material Management Divided in 2 groups:
  - LOG1 - Logistics Warehouse operations;
  - LOG2 - In/outbound and MP Order Desk.
- HRL – Human Resources
  - Implement strategies and accomplish results working as a strategic partner.
- CTG – Controlling Finance
  - Responsible for controlling, reporting and accounting fiscal and legal topics;
  - Provide financial shared services for National Sales Organization and Service Operations, located in Lisbon;
  - Main goal: to guarantee the reliability of the financial information and support the business unit and their customers to take the right business decisions.
- QMM – Quality Management
  - In charge of the implementation, maintenance and continuous improvement of the Quality management system;
  - Monitors the quality performance of the processes, from the industrialization phase to mass production as well as the product quality, environmental and safety performance through the implementation of Quality methods and tools;
  - Implements reliability tests and products audits, ensuring the operational excellence and high level of customer satisfaction.
- TER – Technical Responsibilities
  - Work in the following areas:
  - Process engineering (PCBA);
  - Maintenance (Equipment and Tools);
  - IT (Information Technology);
  - FCM (Facility Management).
- TEF – Technical Function
  - Responsible for the industrialization process within the Plant and supports it in the following areas which support both production and the industrialization process, in order to get the Plant ready for the introduction of newly developed products, from the R& D centers and outside the division:
    - TEF1 – responsible for the development and maintenance of test equipment;
    - MBI (Manufacturing to business interface) – consists of a group of project leaders who ensure the industrialization process;
    - ITM – IT dedicated to manufacture;
    - CoC – Center of Competences; also divided into 2 groups: the first one, PCBA, composed by automatic insertion machines and optical blocks, related to processes inside the cleanroom;

    * Electronics Engineering – Development of production test equipment and Maintenance;
    * Industrialization Process: MBIs (Manufacturing Business Interface);
    * ENI – Engineering Network International - responsible for the product development and support of the development centers.

- MOE – Production management

  The MOE group supports the Ovar Plant in the following areas:

  – MOE1 – SMT with the assembly of electronics boards;
  – MOE2 – Value Stream Video;
  – MOE3 – Value Stream Extreme Video;
  – MOE4 – Value Stream Communication;
  – MOE5 – THT (Through Hole Technology);
  – MOE6 - Industrial Engineering;
  – MOE7 – Value Stream Fire and TT.

- BPS – Bosch Production System
- HSE – Health Safety Environment

1.2.5 ENI – Engineering Network International

ENI is a group integrated into TEF composed by a team of nine mechanical engineers, two component engineers, two product data manager (PDM) and one project manager (PM).

The mechanical engineers are responsible for providing support for products during the production process and developing 2D and 3D CAD design used for simulations testing and production of components. The PDM are responsible for the creation and maintenance of build of materials (BOM), product documents and processing of engineering changes, whilst the component engineers are responsible for the technical analysis, support and approval and follow up of product changes. The PM manages the product lifecycle.

1.3 Thesis outline

The initial structure of the master's thesis is represented in figure 1.6, as well as the organization of the several topics by month in figure 1.7:

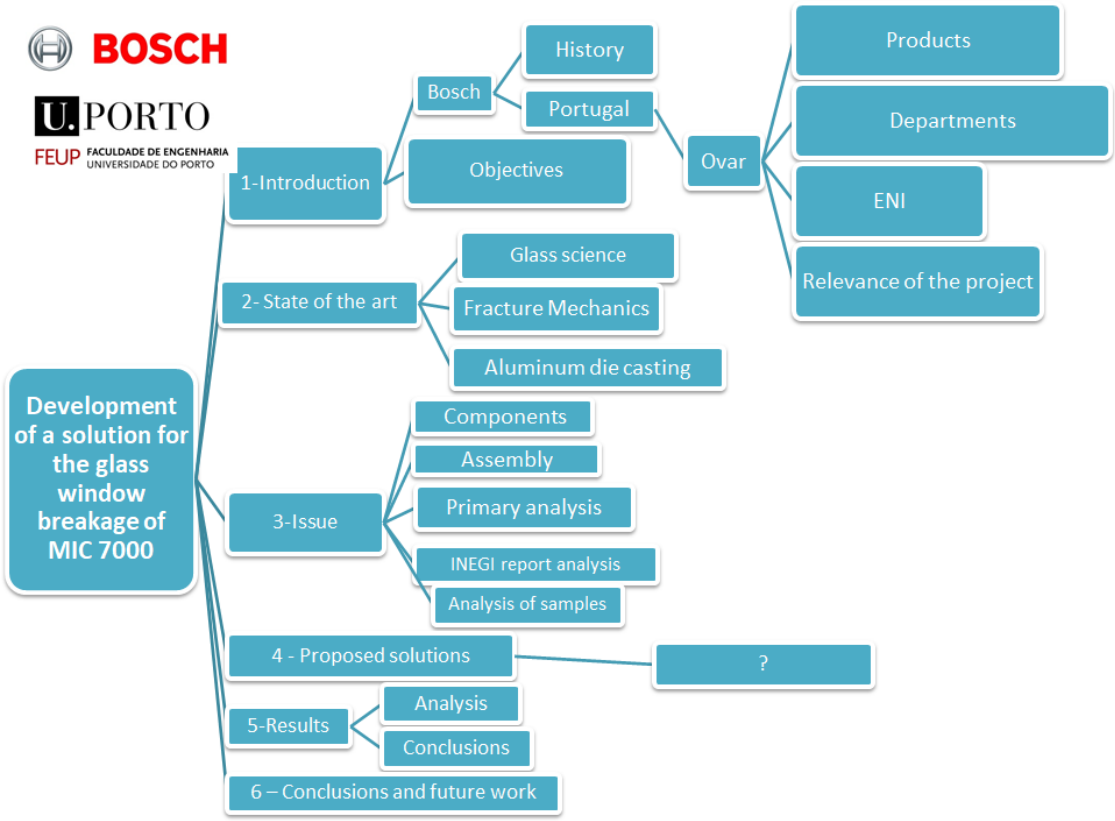

Figure 1.6: Thesis outline

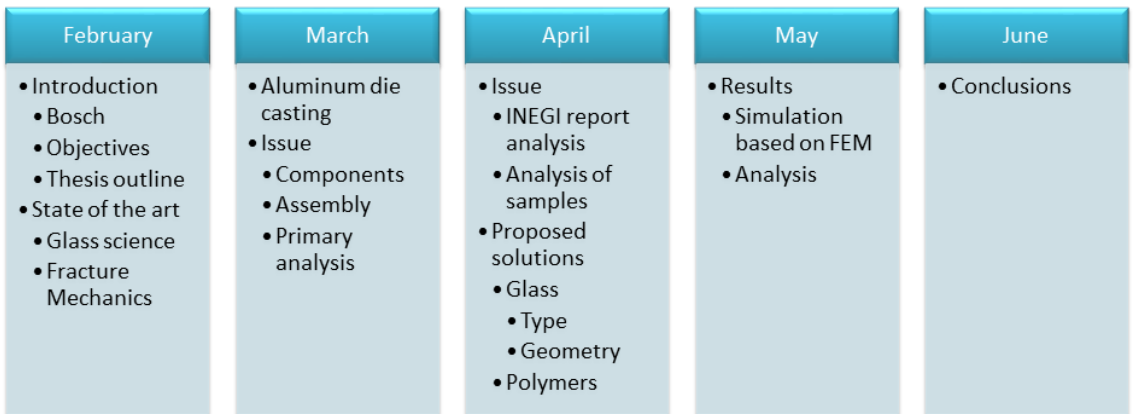

Figure 1.7: Timing

In chapter 2, an intense research about glass science was done so it would be possible to analyze and comprehend the problem: a study about the glass forming process was attained, as well as the mechanical properties, flaws and several methods used to increase its strength, including chemical and thermal strengthening and compressive coatings. Fracture mechanics play also an important role in this project in order to acknowledge the mechanical phenomena and failure criteria which could possibly lead to the window breakageand thus not only the failure mechanisms of glass were investigated but the surface markings were also described. A description of the aluminum die casting process was accomplished in order to better understand the requirements of the proposed solution regarding the manufacturing process.

Then the explanation of the problem is the main topic of chapter 3 where the mechanical properties of the materials were approached and the assembly of the different components in the production line was described. After the first problem approach, which includes a report delivered by Bosch regarding the main information associated with the issue, it was necessary to study the report provided by INEGI where the front shell, the glass window and the other components were subjected to several tests so their stress, strain and deformation could be seen and analyzed in order to find the root causes of this problem. Besides a study on the surface of a sample of the glass was carried out, which came to confirm suspicions about the chemical strengthening process.

Moreover, it was essential to understand what type of glass is being studied and thus in chapter 4 a investigation took place with the main aim of concluding if the type of glass and the chemical strengthening are the more appropriate. The possibiliy of replacing the SLS with a polymer was also analyzed considering a polycarbonate and an acrylic as the candidated for this change. Finally, the glass window geometry was modified so the corners present in the initial geometry were eliminated as well as the residual stress concentration areas.

In chapter 5, the proposals were tested based on the finite elements method in order to conclude if they would suit the company needs.

Lastly, the conclusions of this thesis and possible future work are included in chapter 6.

Chapter 2

State of the art

2.1 Glass science

Glass is an amorphous material, which could mean it has no structure, but actually at the nano-level, it is possible to identify some shapes consisting of rings which contain between three and seven silicium atoms with oxygen atoms acting as bridges between them. These rings are part of a 3-dimensional structure of covalent bonds, which cannot be reformed easily when broken and consequently any local stress around a defect higher than the bond strength can cause bond failure and thus increase local stresses. The absence of a crystal network inhibits dislocations causing also absence of plasticity and therefore glass can only deform elastically or it will break [1].

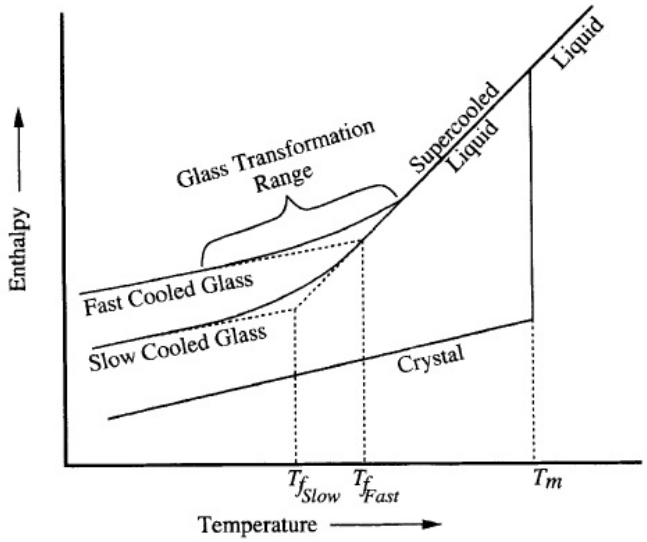

Figure 2.1: Effect of temperature on the enthalpy of a glass forming melt [6]

Regarding the formation process, glass is obtained by melting its components at high temperatures ensuring there is no crystallization. The atomic structure of the melt will gradually change and will be characteristic of each value of temperature. As it can be seen in figure 2.1, if the cooling rate is low enough to achieve a crystalline state, cooling to a temperature below the crystal melting point will lead to the presence of a long range periodic atomic arrangement. In this case, the enthalpy will decrease in a sudden step and the crystalline phase will be in a stable equilibrium. On the other hand, if the cooling rate is superior to the crystals formation rate, a super cooled liquid is attained and the

structure continues to rearrange but with no abrupt decrease in the enthalpy, since the aggregates which form the glass cannot move to attain an ordered structure [7]. The *glass transformation region* is defined as the temperature between the equilibrium liquid and the frozen solid [6].

It is convenient to define a term which represents the indication of the onset of the glass transformation region , i. e., a fictive temperature at which the glass transformation occurs, although it occurs over a temperature range. If the glass and the supercooled liquid lines intersect, the value which is obtained is denominated *glass transition temperature*. This term consists of a useful parameter to discuss the differences in the cooling rate, despite of not being a completely satisfactory concept. Thus, T_g is defined as the *transition temperature*, representing the limit between the state of super cooling and glassy state and it can be considered the frontier between the viscous-plastic state and the rigid state of a glass, the approximate temperature where the solid begins to behave as a viscoelastic solid [6]. A substance at a temperature below this value is referred to as melt, while another at a temperature above T_g is a glass [7].

2.1.1 Glass formation – Soda lime silica

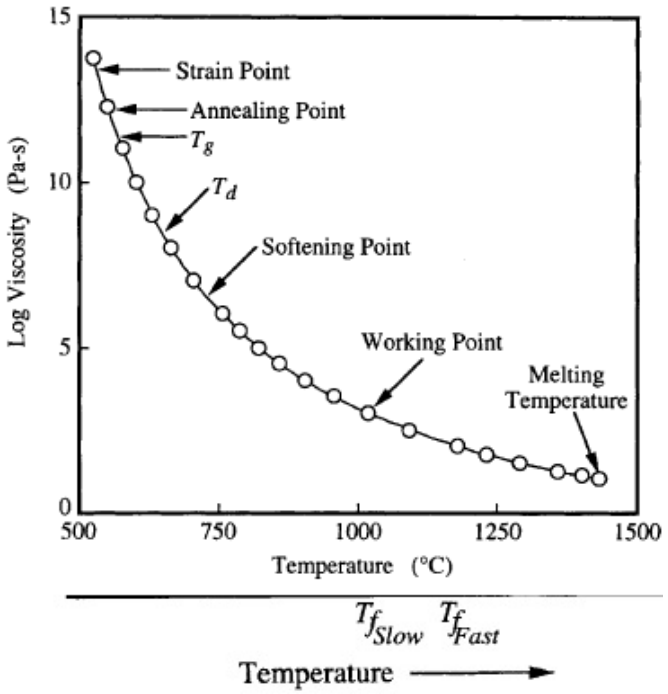

Figure 2.2: Typical curve for viscosity as a function of temperature for a soda-lime-silica melt [6]

A glass object is formed from a melt which requires a shaped viscous amount of liquid – a gob – and fluid enough to preserve its shape after the object is formed. This method demands a big precision in controlling the viscosity during the entire forming process [6].

The working point, presented in figure 2.2, represents the viscosity whose melt is delivered to the processing device - 10^3 Pa.s and the point where its value is sufficiently high in order to prevent deformation owing to the object's own weight is called the softening point, with a viscosity of $10^{6.6}$ Pa.s. The temperature range between these two points is named *working range* and melts whose working range is large are known as long glasses,

whilst the ones with a small working range are referred to as short glasses.

In case the working range occurs at higher temperatures than the working range of a typical soda-lime-silica glass, SLS, its composition consists of a hard glass. However, if the working range is shorter, then the composition is referred as a soft glass. It is important to remember these terms are not related to the resistance of the glass.

After the object is formed, the resultant stresses from cooling are reduced through an annealing process. The annealing point is given by the temperature where the stress is significantly relieved for a few minutes while the strain point is given by the temperature where stress is significantly relieved for several hours, being extrapolated of data from annealing point studies [6]. Float glass is obtained by pouring molten glass on a bed of liquid tin (Sn) in a nitrogen atmosphere where it continuously forms a ribbon which moves from the hot glass over to the annealing lehr and causes solidification, as it can be seen in figure 2.3. Its thickness is dependent on the rate at which the molten glass is poured on the tin. After living it, the glass ribbon is slowly cooled to avoid the formation of residual stresses. There is a high level of control in order to ensure the inexistence of impurities and inclusions as well as internal defects [1].

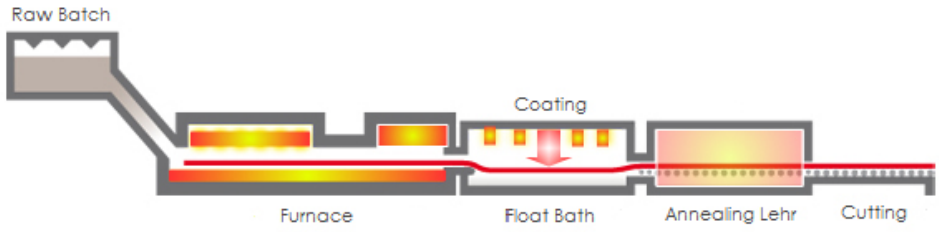

Figure 2.3: Glass formation process [8]

Afterwards the ribbon is cut down according to the desired dimensions, by scratching a line on the glass using a scoring wheel of a elevated hardness. The glass is heated or bent in order to put the scratch into tension, leading to an unstable crack growth, starting from the scratch through the thickness. It is of major importance to select the more appropriate cutting wheel, considering its hardness and cutting angle, as well as the lubricant and pressure. Besides if the plate is very thick the crack growth becomes 3-dimensional which may carry more complications [1].

Regarding the machining process, in order to obtain an even surface the edges are usually ground through a rotary action which removes material, involving cracking the glass into micro fragments, which are washed away [6]. The defects are eliminated and the strength is improved by turning the rough surface into a smooth surface.

Studying the glass science and technology is not a very often task assigned to mechanical engineers, since the main materials they are used to work with are metals, plastics or composites, whose behavior is more easily understood since it is more consistent and simply to predict. However, glass does not work the same way because of its high brittleness and low fracture toughness compared to other engineering materials, in addition to its fracture behavior, which is usually dependent on environmental factors instead of being directly related to the strength of the network bonds [6]. This material is applied in several technological fields such as construction, transportation, aeronautics and electronics, reason why it requires two important properties combined together: hardness and crack resistance [9].

The best way to study and predict glass behavior is to intensely study and analyze its

properties and failure and fracture phenomena.

2.1.2 Mechanical Properties

Starting with the mechanical properties, it is important to acknowledge they depend on several factors: prior surface treatment, chemical environment and presence of surface flaws.

1. **Elastic Modulus**
   E relates an applied force and the resultant alteration in the average separation distance of the atoms that form the material's structure; related to deflection.
   According to Hook's Law, the strain of an elastic material is proportional to the stress applied to it:
   $$\sigma = E\varepsilon \tag{2.1}$$

   Ratio of the transverse strain to the axial strain – υ (Poisson's ratio)

2. **Shear Modulus** G
   Relates shear strain γ^* to shear stress τ through the law:

   $$\tau = G\gamma* \tag{2.2}$$

   The relation between E, G and υ is:

   $$G = \frac{E}{2(1+\nu)} \tag{2.3}$$

3. **Hardness**
   It can be evaluated either through scratch hardness (using Moh's scale) or indentation hardness (using Vickers indenter). Oxide glasses classify from 5 to 7 on the Moh's scale, which means they will scratch apatite (5) but will not scratch quartz (7). The Vickers hardness goes from 2 to 8 GPa, a range significantly lower than diamonds hardness – 100 GPa. Silicate glasses are harder than borate, germinate and phosphate glasses.

4. **Fracture Strength**
   Governs load bearing capacity [10]. Its value can be reduced by surface flaws that strongly weaken the glass, and it is far less than the theoretical strength. Moreover, it is represented as a distributed function instead of exhibiting a single value, based on the variation of the union force between the atoms which is dependent on the distance between them, represented in figure 2.4 [6]:

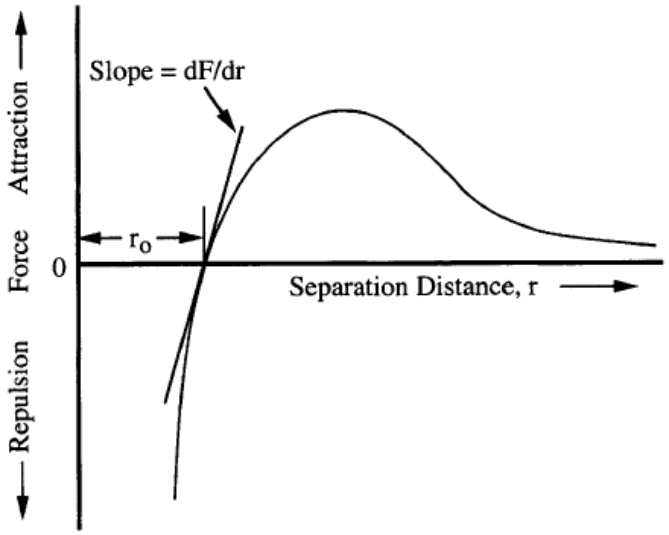

Figure 2.4: Cordon-Morse curve [6]

The Condon-Morse curve represented above leads to the following equation for the force F, as a function of atomic separation distance:

$$F = \frac{-a}{r^n} + \frac{b}{r^m} \tag{2.4}$$

Where a, b, r and m are constant values. The **theoretical strength** represents the force which must be applied to overcome the maximum restorative force. When the interatomic distance overcomes the distance corresponding to the force above, continuously applying the force will extend the bond distance until it is shattered and consequently a crack propagates through the material. According to Orowan, to break a bond it is necessary to obtain the following stress, dependent on the energy necessary to generate 2 new surfaces owing to the fracture:

$$\sigma_m = \sqrt{\frac{E\gamma}{r_0}} \tag{2.5}$$

Where γ is the fracture surface energy and r_0 the equilibrium space distance between atoms. These terms are independent of the glass composition so it is possible to conclude glasses range of theoretical strength is from 1 to 100 GPa, but an ordinary flawless glass presents a theoretical strength of about 35 GPa applied in a tensile mode [11].

Regarding the **practical strength**, its reduction relatively to the theoretical one is due to the existence of surface flaws which act as stress concentrators and increase the local stresses that can lead to fracture. In order to obtain the failure stress, Griffith formulated the following expression:

$$\sigma_f = \sqrt{\frac{2E\gamma}{\pi c*}} \tag{2.6}$$

Where c* represents the critical crack length for crack growth. The larger the flaw, the weaker the structure [12]. In order to obtain a spontaneous crack growth, it is necessary for the stress at the crack tip to exceed the theoretical strength. Besides the Griffith criterion is sufficient to cause fracture since any applied stress that exceeds this criterion will also exceed the theoretical strength [6].

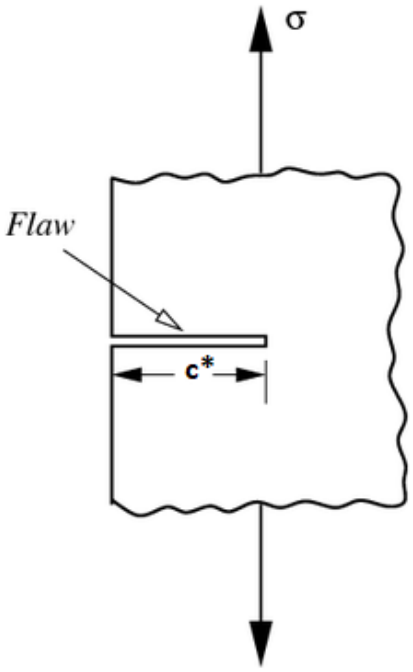

Figure 2.5: Critical crack length [6]

5. **Toughness**
   Governs crack propagation [10], which means it indicates the resistance force to crack extension, or its ability to absorb energy prior to failure [13]. Toughness, K_{IC} is the critical value of a parameter known as stress intensity factor, K_I, discussed later.

2.1.3 Flaws

The contact between the glass and any other material whose hardness is greater can cause a flaw and even contact with another piece of the same glass or with other metal objects, for instance, used to handle it, is sufficient to create flaws.

Moreover, the simple contact with the fingertip will cause flaws because of the deposition of NaCl in its surface and handling introduces flaws generally of the order of 10 to 50 μm[3]. The rapid cooling can also introduce defects through thermal shock as well as heating glass for long periods of time will reduce its strength by forming surface crystals or through the attachment of dust particles to the surface.

There seems to exist some confusion between notches and cracks [14]. A notch can be defined as a geometric discontinuity with a definite depth and root radius and it is an undesirable part of a design: a bolt or oil hole or a screw thread. In a tensile stress field, it can be analyzed through the stress-flow analogy, illustrating the high density of stress around the root of the notch, as it can be seen in figure 2.6.

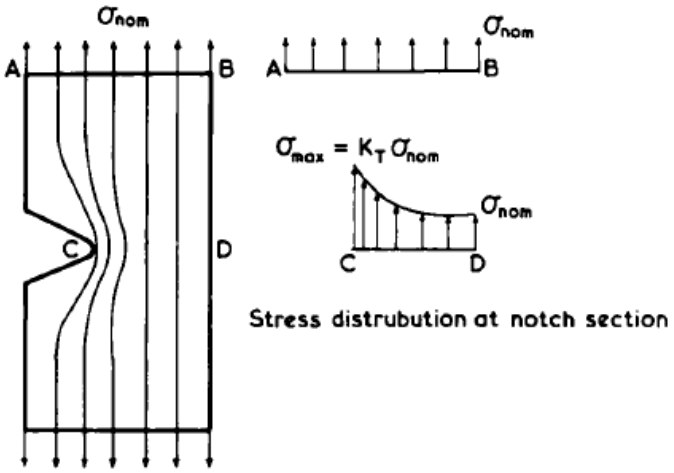

Figure 2.6: Stress distirbution at notch section [15]

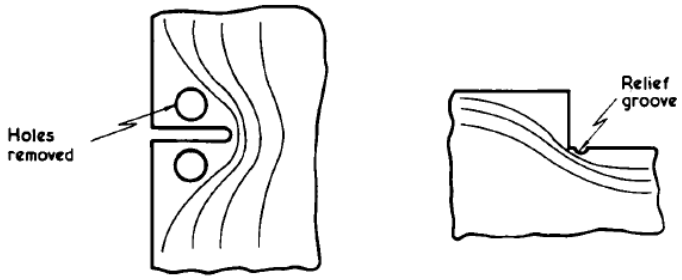

Figure 2.7: "Stress flow" analogy [15]

The modes of crack surface displacement represent the different ways in which a crack can be opened and the extent and shape of the structure which contains the crack:

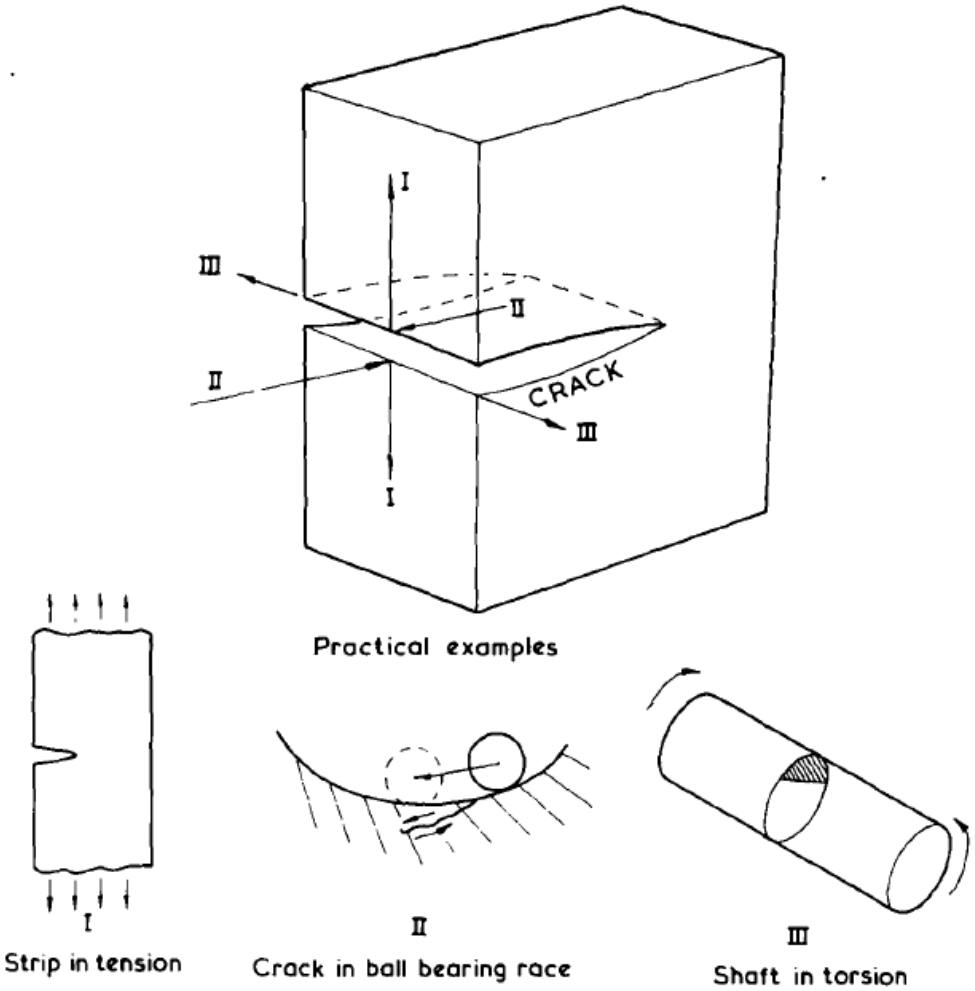

Figure 2.8: Crack modes dispacement [15]

I – opening tensile manner;
II – in plane sliding normal to the crack front;
III – in plane sliding parallel to the crack front.

For each type of displacement, a stress intensity factor can be considered and denoted by the appropriate suffix, I, II, III, according to the respective mode. Mode I type is more commonly found in the literature, despite of great interest in the other modes starts to grow [15].

The geometry of the component should be taken into account since it modifies the value of the stress intensity factor:

$$K_I = \alpha \sigma_i \sqrt{\Pi a} \tag{2.7}$$

σ_i is the uniform applied stress remote from the crack, a is the crack length and α is a geometry correction factor, which is considered 12 % for a semi-infinite half space [15].

In general, in glass the main cause of failure is mechanical contact with glass particles, metals and abrasive grains, during the production or manufacturing processes, or even handling, which leads to conclude the glass with higher crack formation probability would

have a higher risk of cracking during the processes.

2.1.4 Protection

A recently produced glass presents a surface whose coefficient of friction is very high. In order to reduce the introduction of flaws, lubricant can be applied or lubricating coatings which are resistant to wear can be introduced in the surface to prevent the generation of flaws in the underlying glass. In case it happens, they can be eliminated by removing the external surface either by chemical etching or mechanical polishing. Etching consists of blunting the flaw tip and reducing its length but it only results as a temporary increase of glass strength [16]. On the other hand, polishing reduces the length so it becomes below the Griffith criterion and flame polishing consists of using a viscous flow in the near surface to remove the flaws [6].

2.1.5 Strengthening

The big difference between the theoretical and the practical strength has led to several researches with the main aim of improving the first one. This process has two paths: the prevention of the formation of flaws or the removal of the ones that already exist. The latter is not a permanent method since the occurrence of flaws is a continuous process and impossible to completely avoid, reason why the main focus should be on preventing crack growth by introducing a compressive layer in the glass surface. In order to do so, three options can be considered: compressive coatings, thermal tempering or chemical strengthening [17].

Compressive stress coatings have a lower thermal coefficient of expansion than the glass. These coatings can be applied at two stages: hot end coatings take place just after the glass left the forming machine and before entering the annealing lehr; cold end coatings are applied immediately before it leaves the lehr and can be applied as a vapor or by spray. The first ones are made of tin or titanium while the latter include organic waxes, polyethylene emulsions or glycols [18].

Thermal tempering is given by the rapid cooling of the glass surface from at or above the upper limit transformation range. Because the internal glass will cool more slowly, the equilibrium density will be bigger than the one from the surface region, meaning the glass is cooled so rapidly from a temperature in the softening range that before the glass object as a wbole has reached a temperature below the transformation range, a temperature gradient is formed [19]. This process is not very efficient in very thin wall or fibers applications since the difference in the cooling rate is small as well as in vitreous silica or commercial borosilicate glasses, because of their low expansion coefficient. Even so the commercial strength glass market is essentially dominated by thermal tempering because of its ease of application (hence cost-effectiveness) and its relative forgiveness to handling flaws due to mostly, for instance, the nearly 1 mm “case-depth” (depth of compression layer) in a 5-mm wall thickness, as it is discussed by Varshneya.

Chemical strengthening consists of exchanging small ions such as Li^+ or Na^+ in an alkali-containing glass for larger ions like K^+ in an electrically heated molten salt bath (below the annealing point), resulting on the generation of a residual compressive stress in the surface layers of the material, since the invading ions (K^+) are larger than the host ions, as it presented it figure 2.9. This interdiffusion of ions is able to increase the strength by 2 or 5 times and it takes place at temperatures above the strain point of glass, although

the exchange of a small ion from the glass by a larger one from at a temperature below the transformation range can also lead to high compressive stresses, despite of the very thin compressive layer achieved [19]). The compressive stress layer has to be deeper than the existing cracks, in order to increase strength [17].

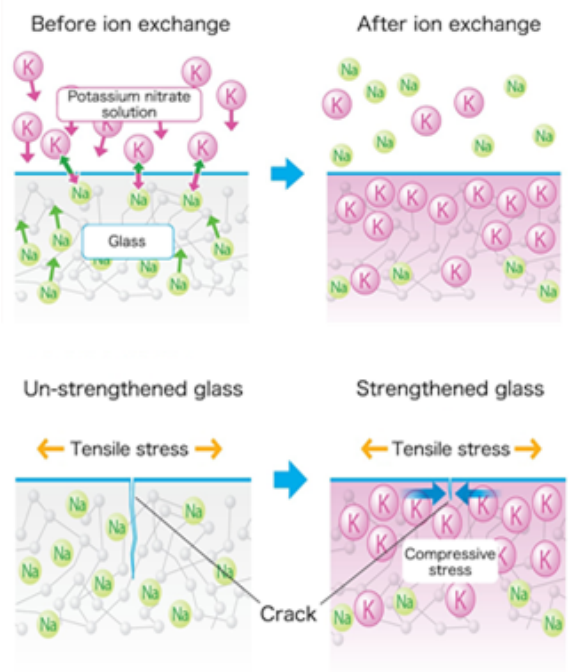

Figure 2.9: Ion exchange process [20]

This process depends on temperature and time since it is a diffusion-controlled process and therefore the higher the temperature, the shorter the time needed to generate a layer of compression stresses. According to Fick's second Law, the thickness of ion exchange layer is proportional to $\sqrt{t}$, having t as the time of immersion in the potassium nitrate molten bath and the compressive stress resultant from the ion exchange increases with the increase of the immersion time [21]. The upper temperature has a limit, T_g, owing to the phenomenon of stress relaxation, since the stresses created by this process are rapidly relaxed or even eliminated if ion exchange is carried out at a temperature above the glass transition temperature T_g or for long periods of time [21]. Thus, chemical strengthening may take only a few minutes or several hours, according to the glass composition, bath temperature and case depth [22].

Concerning the advantages of this process, it is possible to conclude that beyond the introduction of a high surface compression, it also encases no measurable optical distortion, thin plates (even less than 1 mm) and the possibility of strengthening irregular geometry products, as long as the surface can be contacted by the molten salt [23]. On the other hand, chemical strengthening is limited to alkali-containing glass, the glass is susceptible to weakness when it comes to soda-lime glass, because of its low case depth and it can be quite expensive owing to extended bath immersion [11].

Chemically strengthened glass is suitable for transparent armor, hurricane-resistant, architectural windows, solar energy collector substrates [11], autoinjector cartridges to prevent anaphylactic shock and aircraft cockpit windshields [23].

2.1.6 Fatigue

Static fatigue is defined as the decrease of the strength of glasses with time in normal ambient conditions owing do their interaction with the surrounding atmosphere having as a result crack growth under constant load. *Dynamic fatigue* occurs when the load is rapidly increased, and consequently the failure strength is higher, usually under conditions of changing load [6].

2.2 Fracture mechanics

Fracture mechanics consists of a group of theories related with the behavior of structures containing geometrical discontinuities at the scale of the structure which can take place in either two-dimensional media, such as plates and shells or in three-dimensional media. Its development is strongly related to the occurrence of disasters through history, for instance, fractured ships during World War II, whose root causes were mainly associated to poor weld properties resulting in stress concentrations and also poor choice of brittle materials throughout the construction [14].

This field can be divided into linear elastic fracture mechanics (LEFM), which is indicated to brittle-elastic materials, such as steel, glass, ice and concrete, and elasto-plastic fracture mechanics (EPFM). On the other hand, in low-carbon steel, stainless steel, some aluminum alloys, polymers or other ductile materials fracture will only occur after plasticity. Even so if an applied load is low enough to analyze the linear domain, it can be a good approximation to the physical reality [14].

The strength of a component or structure which contains defects can be defined through the evaluation of the stress concentration resultant from the discontinuities. The "stress flow", where the effect of a notch on a tensile stress field is represented (figure 6), can be very useful in deciding upon the course of action – either removing or adding material to smooth out the flow stress. If the material is removed in case 4 (figure 2.10), with a width equal to a, then the loss of strength in cases 3 and 4 can be recovered to the same level as in case 1 [15].

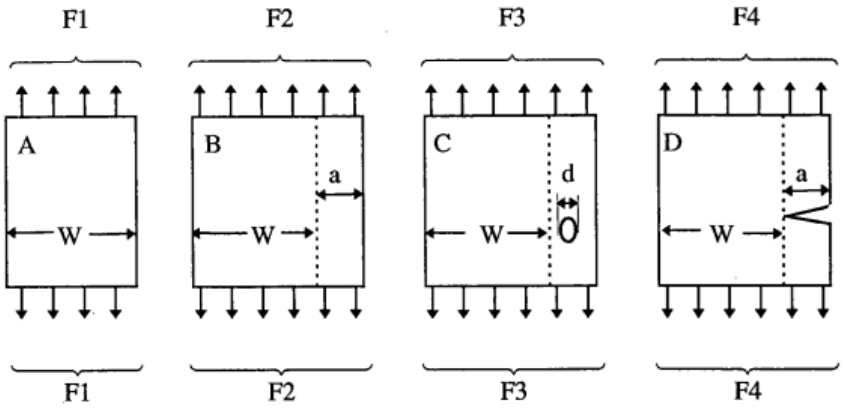

Figure 2.10: Strength of uncrack and cracked plates [14]

In 1920, as mentioned above, Griffith identified flaws as the nuclei of fracture and was able to conclude the strength of a brittle material with a slender elliptical through crack of size $2c$ in a uniformly stressed plate in plane stress plane is given by σ_f, the fracture

stress.

The stress concentration factor K_T is defined as the dimensionless ratio of the maximum (elastic) stress at the root of a notch to the nominal applied stress and reflects the severity of a notch [14]

$$K_T = 1 + 2\sqrt{D/\rho} \tag{2.8}$$

Where D is the notch depth and ρ the notch root radius, meaning if a circular hole is being analyzed, K_T is 3, since the notch depth is equal to the root radius. For common notch shapes the K_T value can be obtained from tables and charts. The presence of a notch strongly affects the safety of structures made of brittle materials.

When ductile materials are analyzed, it is possible to conclude notches are less dangerous, because the stress gradient ahead of a concentrating feature is steep, and consequently limits the spread of plasticity to a small region, simultaneously avoiding plastic collapse [15].

2.2.1 Failure criteria

Stresses at the crack tip that exceed yield result in plasticity, but if plasticity is minimal, a LEFM approach is still sufficient accuracy for engineering applications.

The amount of energy absorbed in plastic deformation is reduced to a minimum range and much more energy is left for fracture. The critical state is described by the condition of the stress intensity factor equalizing the material's toughness [14]:

$$K_I = K_{IC} \tag{2.9}$$

Concerning a truly brittle material, such as ice or glass, the energy for crack growth is the surface energy needed to form a new surface:

$$G = 2\gamma \tag{2.10}$$

where the factor "2" represents the two crack surfaces which are being created. Nonetheless the energy required for crack growth in an engineering material is much greater than the surface energy, due to plastic deformation occurring near the crack tip region, where during crack extension, energy is consumed by plastically deforming the material. This criterion can be presented as [14]

$$G = 2W_f = 2(\gamma_f + \gamma_p) \tag{2.11}$$

Where γ_p is defined as the plastic work per unit area of surface created, usually larger than γ_f, the natural surface energy [45]. 2 W_f generally is conveniently replaced with R, representing the material resistance to crack growth as well as having a plot of R versus crack extension, denominated R-curve or resistance curve. This curve is a material property dependent on temperature, loading rate, etc. The majority of the brittle materials present a constant resistance called "no R-curve" effect, as illustrated in figure 2.11, where two loading scenarios, σ_1 and σ_2 are considered. The resistance to crack propagation, R, is contant, so the crack will not propagate until the critical energy release rate G_C is attained and in case 2, it is necessary a shorter crack to lead to propagation, comparing to situation 2 [24]. The shape of the R-curve is related with the material and with the configuration of the cracked structure [14].

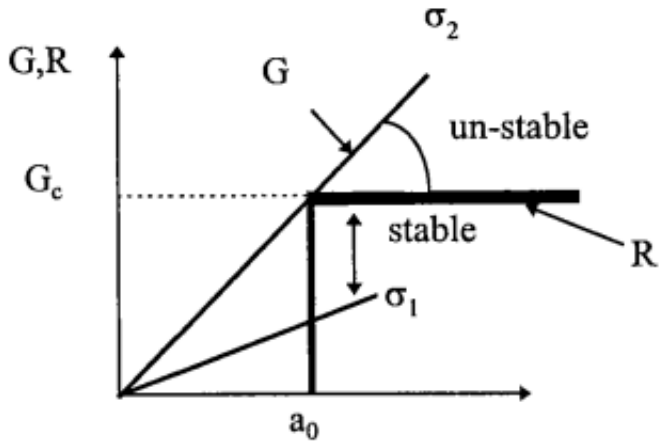

Figure 2.11: R-curve (crack resistance curve)for a glass [14]

2.2.2 Glass fracture

Firstly, it is important to understand glass breaks under tension, since the compressive strength of glass is quite higher than the tensile strength. Glass deforms elastically until the elastic limit on the opposite side from where the force is applied is reached and therefore the fracture initiates in this side, whilst the near side is under compression. The tensile limit will be reached before the compression limit, meaning glass may break under compression, but it has already broken under tension [25].

Besides it is already known the phenomena associated with breakage is crack propagation by tensile stress concentration at a damaged point on the glass, a flaw, which acts as the origin of the breakage. In order to eliminate breakage factors, it should be possible to identify its origin and to reduce the concentration stress. The analysis of the glass surface can be an effective manner of developing a theory about this issue.

Surface markings

By reconstructing the fracture mechanism, it has been possible to study glass fracture through the analysis of some surface markings, since when glass is broken, "footprints" of cracks are memorized on the surfaces, which map the fracture event and are related to its origin, crack propagation and also with the stress applied [25]. Fracture analysis is divided into two parts: obtaining information from the glass surface (forking, chatter mark, residue) and obtaining information from the fracture surface (Waller lines, Hackle marks, mirror region...). The surface topology, which can be characterized by these markings such as Wallner lines, Hackle marks, fracture patterns (radial, concentric or conchoidal), etc., will be briefly described below [26].

Forking indicates crack branching and only provides information of qualitative nature, since it is only possible to conclude about the magnitude of the applied stress from the number of cracks forking, as illustrated in the following figure:

Chatter marks are created by friction mechanisms, while its concavity indicates the friction direction.

Residue can bring information regarding the material which the glass has been in contact with [26].

Regarding the fracture surface, it is possible on identify several features and conclude

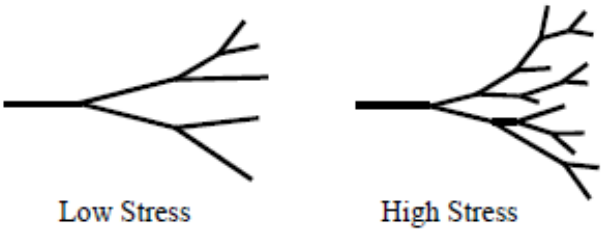

Figure 2.12: Forking with high and low stresses [26]

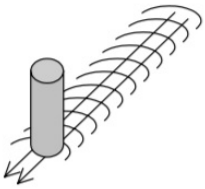

Figure 2.13: Chatter marks [26]

different aspects related to the direction of crack propagation, type of stress, location of the origin, as shown in figure 2.14:

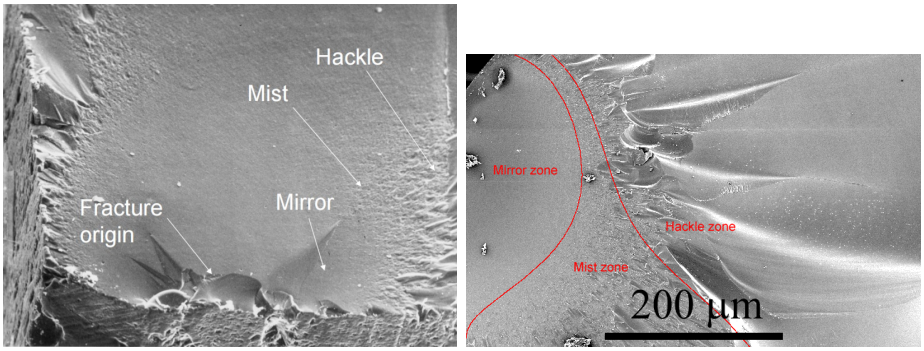

(a) (b)

Figure 2.14: Features present in a glass surface [27] [28]

The mirror region is located near the fracture origin, containing the area where the crack propagation is relatively slow and may be more or less extensive according to the intensity of the impact force, since it only exists for a few millimeters when the impact is moderate, but it may occur for several centimeters if the impact force is very low. Its name is due to its flatness, which reflects light, and it can be observed in figure 2.15.

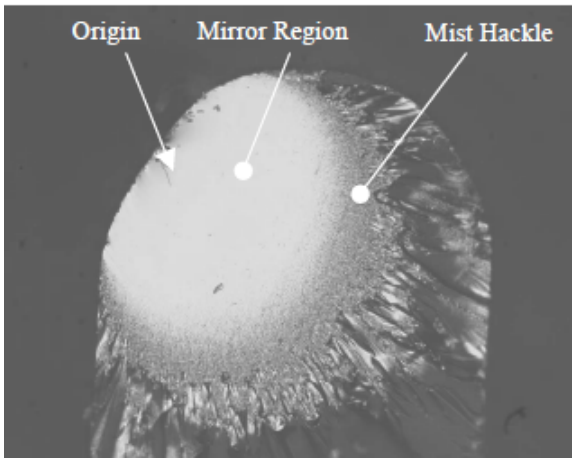

Figure 2.15: Origin, mirror and mist [26]

Mist is a region containing very small cracks due to the increase of the surface area by the fracture tip, which cannot dissipate the accumulated stress efficiently. This region concentrically surrounds the mirror region [29].

Hackle marks are still a subject of some controversy in the engineering literature since it is not clear if they result of the reduction of surface free energy or if they are formed on a surface owing to a localized realignment as an effort for the crack propagation to remain perpendicular to the tensile stress [25]. Is it a rough, ridged region of tensile fracture surface following the mirror and mist regions.

Wallner lines (also called conchoidal lines) consist of arcing lines on the fracture surface of broken glass and are related to direction of the force applied. The relevance of these markings is quite considerable and greater than the ones previously discussed. These lines result from small perturbations in the crack path, normal to the plane of the crack, caused by stress waves created by the crack. If the analyst knows the nature of the conchoidal fracture, whether it is a radial or a concentric fracture surface, it is possible to determine the direction of application of force. As shown in figure 2.16, a radial fracture emanates from the point of impact (1) while a concentric fracture is formed around the point of impact in a circular pattern (2).

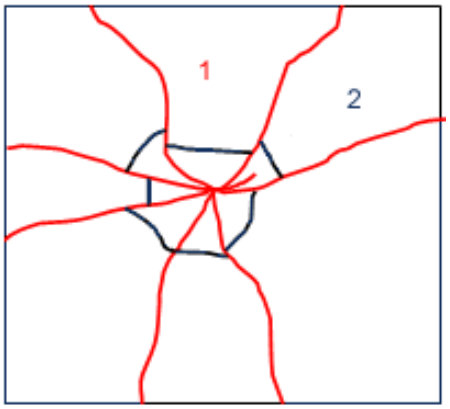

Figure 2.16: Radial and concentric fractures [30]

If a piece of glass presents a radial fracture, then the lines intersect the opposite surface on which the force was applied at right angles, whereas a concentric fracture

surface exhibits the same features but on the same side of the force of impact.

When a force pushes on one side of a float glass, it bends on the direction of the applied force and once the elastic limit is reached, the glass begins to crack on the opposite side, since it is the side which is under tension. As presented in figure 2.17, the first fractures develop into radial lines whilst continued motion results in tension on the surface where the force is applied, creating concentric cracks, due to the fact that the kinetic energy transferred to the glass cannot be relieved by the radial fractures alone [31].

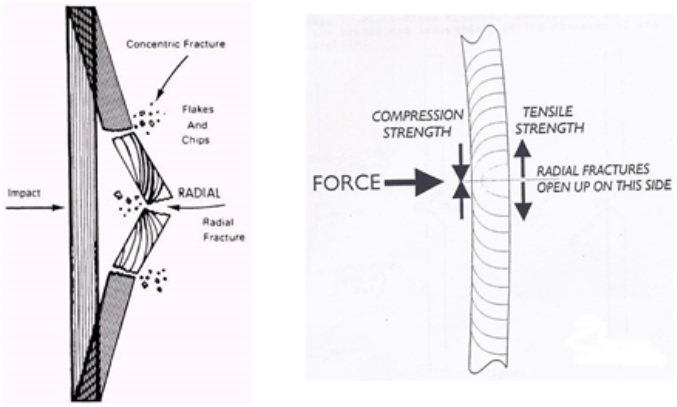

Figure 2.17: Radial and concentric fractures [32]; Compressive and tensile strength [33]

Besides, fractures do not cross: a fracture approaching another fracture will be quickly arrested and will not extend beyond the first fracture, since the continuity of glass has been disrupted by the first one, and therefore inhibited the second fracture from keeping any further, which permits the determination of a temporal sequence in the comparison of two fractures. It is possible to verify in figure 2.18 the left fracture preceded the right one [31].

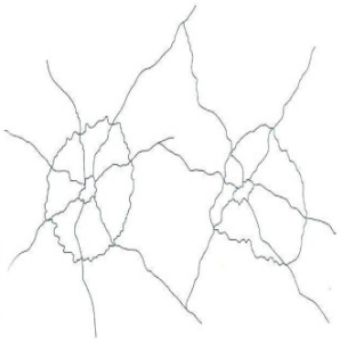

Figure 2.18: Fractures not crossing [31]

2.3 Aluminum die casting

In order to correctly understand the behavior of the shell, it becomes necessary to do a previous overview of aluminum die casting, including the description of this manufacturing process, its requirements and main applications.

Die casting consists of a manufacturing process in which molten metal is poured into steel molds – known as tool or dies – which are specially designed for the component, in

order to obtain accuracy and repeatability in the final product.

The most commonly used alloys in die casting are zinc, magnesium and aluminum which present good corrosion resistance, high strength and hardness, high thermal and electrical conductivity and good finishing characteristics.

Aluminum alloys are lightweight and able to withstand the highest operating temperature of all die cast alloys. They exhibit outstanding corrosion resistance, very good strength and hardness, good stiffness, full recyclability, good dissipating properties, maintains high dimensional stability with thin walls and can be used in almost any industry [34].

There is more than one concept inside the die casting process: hot chamber, usually used for low-melting alloys such us magnesium or zinc, and cold chamber, better suited for aluminum alloys due to their high melting points.

2.3.1 Advantages and limitations

The main advantages of this process are related to the dimensional accuracy present in near-net-shape parts, the complexity of geometry, the possibility to obtain consistent properties which meet specified requirements and to the controlled surface finish. Besides, it is possible in some cases to replace several welded components or joined assemblies with a single cast part and the machining requirements are significantly reduced. Tighter tolerances and fast cycle times can be attained [34]. It is also possible to highlight the differences between as-cast and machined finishes in order to attain cosmetic effects and most aluminum casting alloys present solidification characteristics compatible with foundry requirements for the production of quality parts, which are often cast by every known process, exhibiting a large range of volume, productivity, mechanization and specialized capabilities. Several aluminum casting alloys also offer excellent fluidity which lead to obtain thin sections and fine detail and melt at relatively low temperatures [35].

On the other hand, there are some practical limitations in size and solidification behavior regarding specific casting processes or difficult engineered configurations, since for instance, very thin sections may not be castable, and the solidification in complex shapes can result in surface discontinuities which affect properties, performance and consequently quality.

2.3.2 Cold chamber

This concept is ideal for metals with high melting points and corrosive properties, which would damage the pumping system of a hot chamber machine. Besides aluminum, brass and magnesium can also be included in this concept. While the hot chamber machine contains the melting pot, the cold chamber melt pot is separate and the molten metal is transferred by ladle, manually or automatically into the shot sleeve, having the metal held temporarily in a container. The injection piston forces the metal into the die in a single shot operation, minimizing the contact time between the molten metal and the injector components and consequently contributing to extend their operating life, presented in figure 2.19. The typical values for the injection pressures regarding a cold chamber process are between 2000 and 20 000 psi (14 to 140 MPa).

The first step involves the preparation and clamping of the halves of the die where each one of them is cleaned and lubricated to facilitate the ejection of the part, which can only be needed after 2 or 3 cycles. Afterwards the two halves and are attached inside the

machine and securely clamped [34].

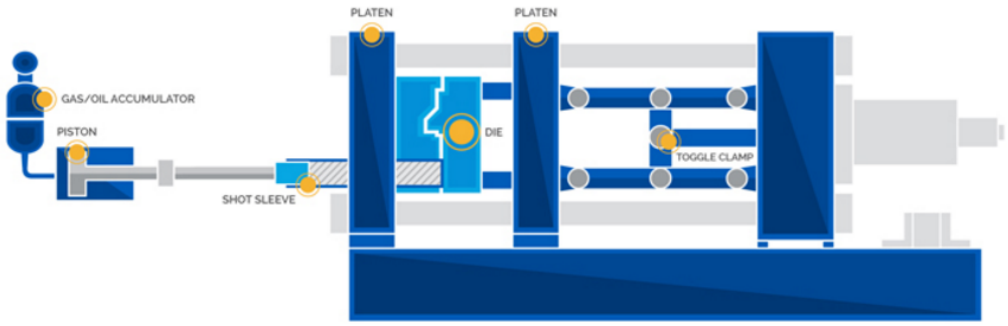

Figure 2.19: Cold chamber process [34]

In the figure 2.20, it is possible to verify firstly the molten metal being poured into the shot sleeve by a ladle, and secondly the plunger pushes the molten metal into the die cavity. Here it is held under pressure until it solidifies. The amount of metal injected into the die is denominated shot and the injection time consists of the time required for the molten metal to fill all the channels and, which is typically less than 0.1 s, so early solidification of any part is avoided and it is dependent on the thermodynamic material properties and on the wall thickness of the casting: a large wall thickness requires a longer injection time. Considering a cold chamber die casting machine, the injection time must include the time to manually ladle the molten metal in the shot chamber. There is extra material than it is required in the molten charge and it is used to force additional metal into the die cavity to compensate for shrinkage phenomena occurring during solidification [36].

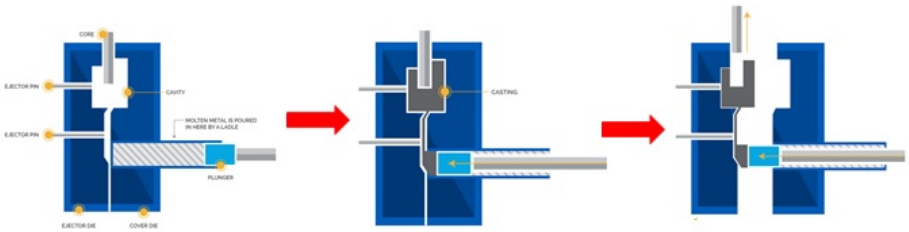

Figure 2.20: Cold chamber: injection step [34]

The die cannot be opened until the cooling time has passed and the casting is solidified in order to ensure the final shape of it is formed. Analogously to the injection time, the cooling time can also be determined from thermodynamic properties of the metal and the maximum glass thickness of the casting, as well as the complexity of the die. Both a greater wall thickness and a geometric complexity require a longer cooling time due to the additional resistance to the flow of heat [36]. Afterwards, the die opens and advances in order to guarantee the casting remains in the ejector die. At last, the ejector pins push out the casting of the other ejector half and the plunger returns to the initial position.

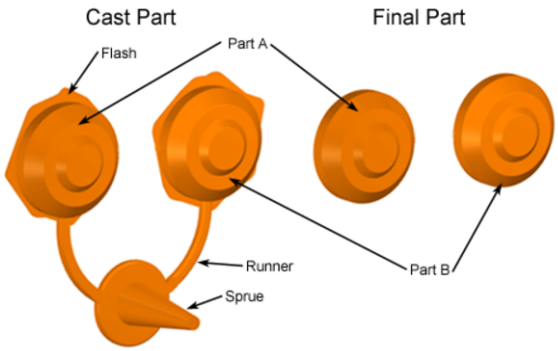

Figure 2.21: Trimming of the excess material [36]

The last step involves trimming the excess material along with any flash, either manually or cutting it, as it is presented in figure 2.21. The scrap material can be reused in the die casting process or it can be discarded. In the former case, it might need to be reconditioned to the required chemical composition before being combined with non-recycled metal and applied in the die casting process.

2.3.3 Design rules

Regarding the maximum wall thickness, decreasing it will reduce the cycle time (injection and cooling time specifically:

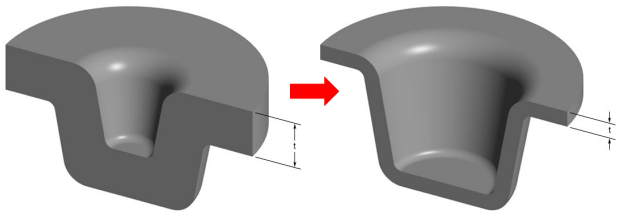

Figure 2.22: Components with inappropriate thickness [36]

On the other hand, a uniform wall thickness will ensure uniform cooling and decrease defects:

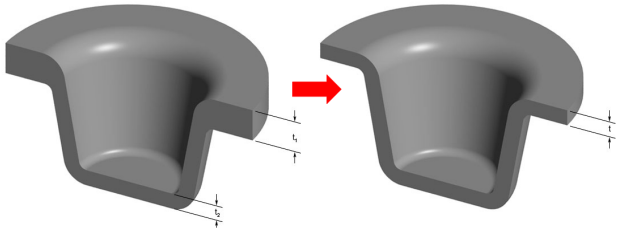

Figure 2.23: Component with a uniform thickness [36]

The corners should be round in order to reduce stress concentration areas and fracture and the inner radius must be at least equal to the thickness of the wall:

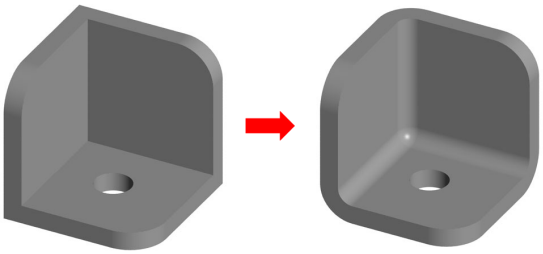

Figure 2.24: Rounded corners [36]

A draft angle should be applied to all the walls parallel to the parting direction so the part is easily removed from the die. Regarding an aluminum alloy, 1º for the walls and 2º for inside cores:

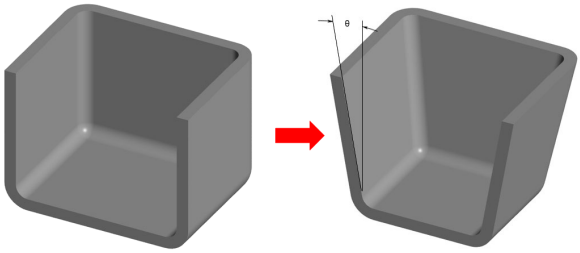

Figure 2.25: Drafts [36]

A few examples of parts obtained from aluminum die casting are engine cooling fans, camera chassis and gaming headsets, presented in figure 2.26:

Figure 2.26: Parts obtained from aluminum die casting [34]

Chapter 3

Issue

3.1 Introduction

The product MIC7000, a camera suitable for outdoor, industrial or commercial surveillance was introduced on the market in 2014, in the second semester and it is produced in Bosch Security Systems, in Ovar. Since then breakage of the glass window has been happening becoming a problem during the production process. At first, the breakage numbers were very low; however an increase in the rejection numbers was verified during the first semester of 2016, which led Bosch to intervene and to start a project alongside with FEUP and INEGI in order to search for the root causes of the window brakeage. The aim of this master's thesis is to propose design and structural changes to the product parts that could eliminate or minimize the breakage risk.

Figure 3.1: MIC 7000 [5]

The glass window breaks preferably in both 1st and 4th corners, mainly the 4th one, which would possibly indicate there is a stress concentration region along this diagonal. Besides this failure is usually found when the components assembly is being done in the workstation, either while the product is waiting for the process or when the leakage test is already being executed.

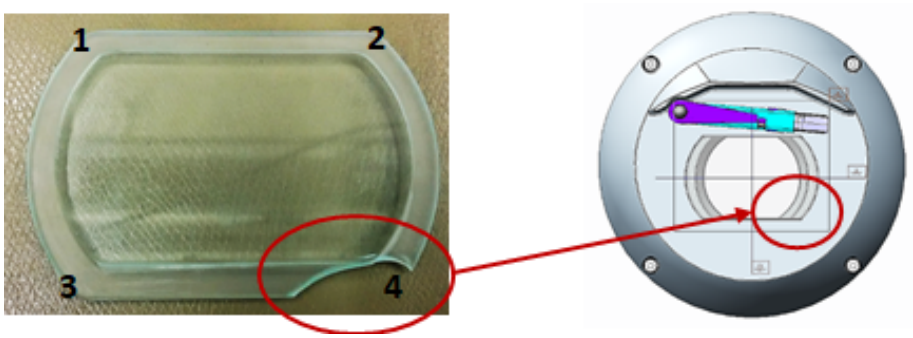

Figure 3.2: Glass window breakage

The problem stabilizes during a few periods of time but can increase without a known explanation, reaching a critical value of 90 % in June 2016, as it can be seen in the following chart.

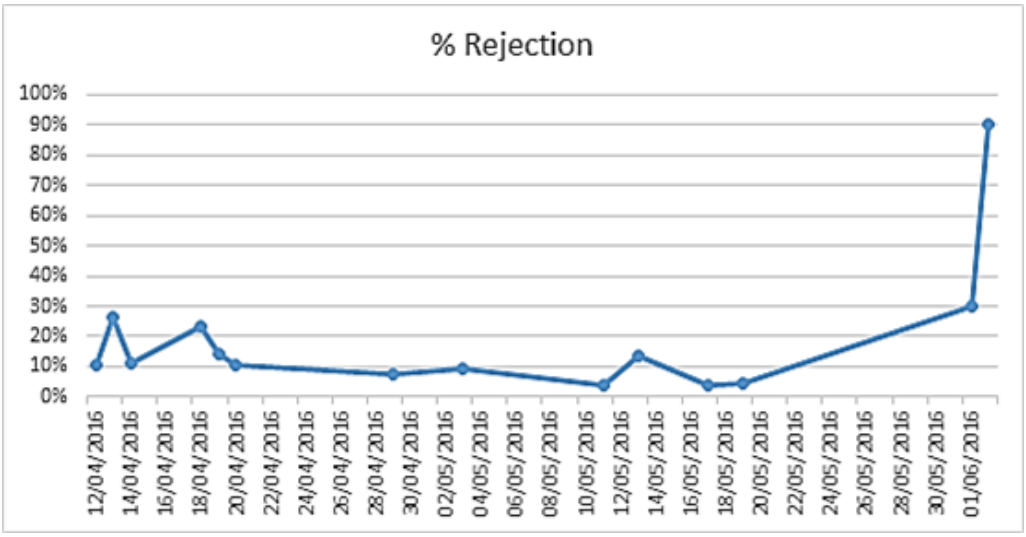

Figure 3.3: Glass window rejection

3.2 Components

The components which intervene in the assembly process, being directly related to the problem are the front shell, the bezel, the gasket, the mylar and the glass window.

3.2.1 Front shell

The shell is the larger component of the camera, the one who keeps all the internal parts safe, such as small pieces, electrical wires, the lens, the wiper engine, etc. It is also in the shell that all the other components directly intervenient in the main issue are assembled: it contains a small window where the glass is placed, as well as all the other components, such as the gasket, the insulator and the bezel.

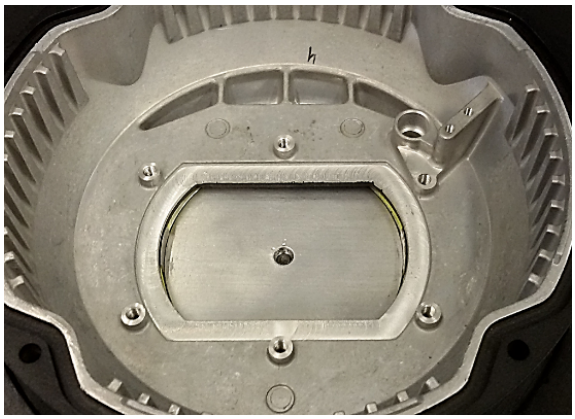

Figure 3.4: Front shell

It is made of an aluminum alloy (AC-AlSi12) and obtained from die casting. Afterwards it is machined, using the milling process: first in the surface where the gasket is placed (green) and then in the top surface of the bosses (red), represented in figure 5.

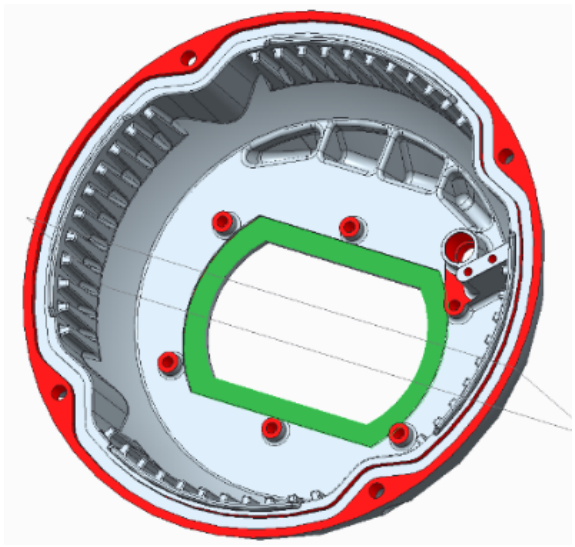

Figure 3.5: Front shell

The composition of the aluminum alloy is presented in table 1:

The aluminum mechanical properties presented in the following table are considered for both the shell and the bezel:

Table 3.1: Chemical composition of aluminum alloy

Constituents	Composition
Al	84.4 - 89.5
Si	10.5 - 13.5
Fe	0 - 0.65
Mn	0 - 0.55
Ti	0 - 0.2
Cu, residuals	0 - 0.15
Pb, Mg, Ni	0 - 0.1

Table 3.2: Mechanical properties of the aluminum alloy

Property	Value
Density (kg/m^3)	2700
Young Modulus (GPa)	81
Tensile Strength - Ultimate (MPa)	180
Tensile Strength - Yield (MPa)	88
Poisson's ratio	0 - 0.33

This component is finished with a porosity sealant and afterwards it is painted with a base coat, a primer and a topcoat.

3.2.2 Bezel

The bezel is a connection part, since it is assembled to the front shell to guarantee the glass window is attached to it, through the application of 6 screws. Besides it also blocks the view into the interior.

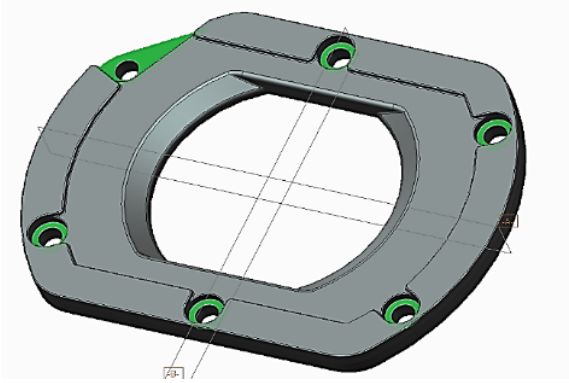

Figure 3.6: Bezel

It is also an aluminum component made of the same alloy as the front shell, obtained from the die casting process, and it has the same mechanical properties as the front shell, already presented.

3.2.3 Gasket

This component works as a sealant, its main aim is to ensure the watertightness inside the front shell and it is made of a silicone rubber – KE-941U.

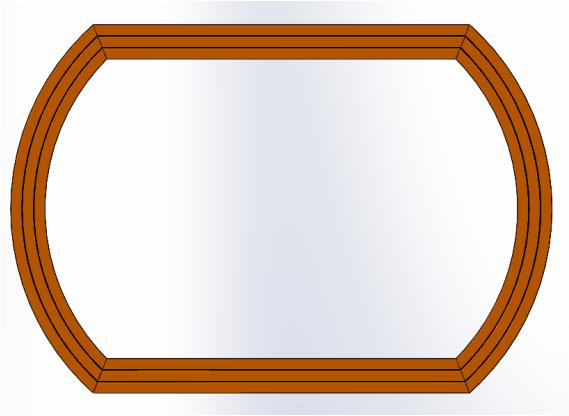

Figure 3.7: Gasket

The mechanical properties were provided by the supplier and they presented in table 3, although there is no information regarding some of them, such as the Young Modulus and Poisson's ratio.

Table 3.3: Mechanical properties of the silicon rubber

Property	Value
Density (kg/m^3)	1110
Hardness Durometer A	43
Tensile Strength (MPa)	6.5
Elongation at break (%)	365

3.2.4 Insulator

In case of the presence of impurities in the bezel's surface, there is a component playing the role of precluding the contact between the glass window and the bezel – the mylar window insulator. It is made of a mylar sheet 0.125 mm thick. The mechanical properties of this component were not provided by the supplier.

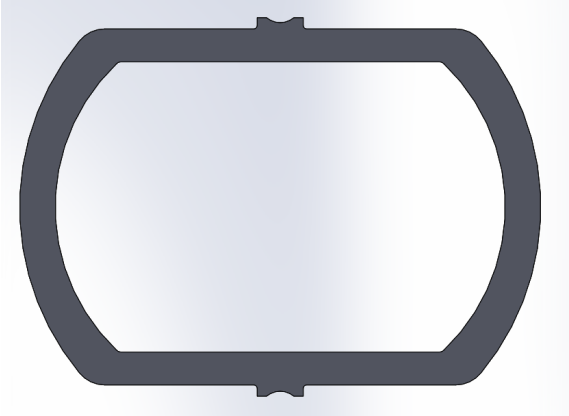

Figure 3.8: Insulator

3.2.5 Glass window

Concerning the glass window, it consists of a clear soda-lima-silica glass, meaning, as mentioned above, it contains alkaline earth oxides and alkali oxides with the composition below:

- 10-20 % alkali oxide – soda (Na2O);
- 5-15 % alkaline earths – lime (CaO);
- 70-75 % silica.

The chemical composition is also presented in table 4.

Table 3.4: Chemical composition of the soda lime silica glass

Constituents	Composition (%)
SiO_2	72.6
Na_2O	13.9
K_2O	0.6
Al_2O_3	1.1
CaO	8.4
MgO	0 - 3.9
SO_3	0.2
Fe_2O_3	0.11

This component has the main aim of protecting the camera lens and simultaneously ensuring the video quality is not compromised, since it should be a strong piece, resistant to the environment conditions. It is made from the process mentioned in the glass science chapter and machined through the grinding process. Afterwards an ammonium bifluoride solution, an acid etching, is applied to the edges in order to remove possible surface flaws and prevent strength degradation and later it is chemically strengthened based on the ion exchange process, in a potassium nitrate bath, whose case depth of 30-50 μm is specified in the drawing.

The glass window is the critical component, since it is the one which breaks, mainly it the 1st and 4th corner, despite of all the corners present residual stress concentration, as it will be later analyzed and explained. In the following figure, it is possible the verify que preferred corner where the glass breaks:

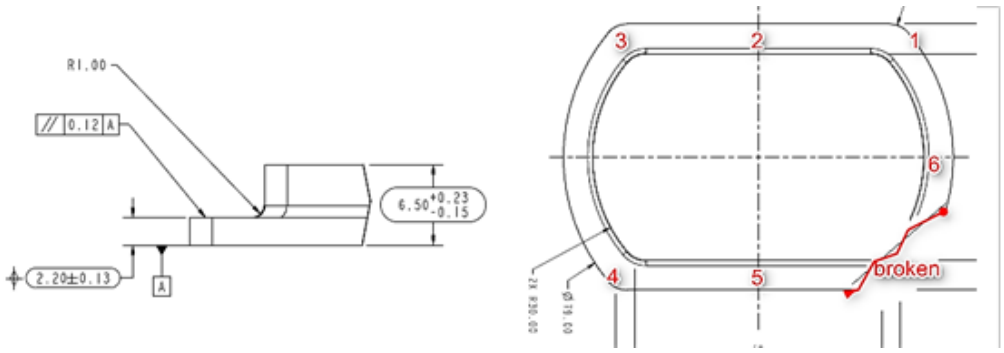

Figure 3.9: Preferred corner and dimensional tolerances

The mechanical properties provided by the supplier are also here exhibited:

Table 3.5: Mechanical properties of soda lime silica glass

Property	Value
Density (kg/m^3)	2530
Young Modulus (GPa)	72
Poisson's ratio	0.23
Hardness (Mho's)	5-6
Tensile Strength - Ultimate (MPa)	41-180

3.3 Assembly

The production of MIC7000 is accomplished in the factory, in line 19 specifically. All the components are received from several suppliers and assembled in different steps. The ones chosen here to be described are the steps directly related to the present issue, and a careful analysis was made in order to ensure the assembly is being correctly done.

Figure 3.10: JIG

Firstly, in order to obtain a good fixation, the front shell and the glass window are assembled in a JIG, which also ensures the central position of the window relatively to the front shell.

After having the front shell fixed in the JIG, the gasket is inserted in the shell, the glass window is cleaned with the air gun and placed on top of the gasket while the mylar is positioned on top of the glass.

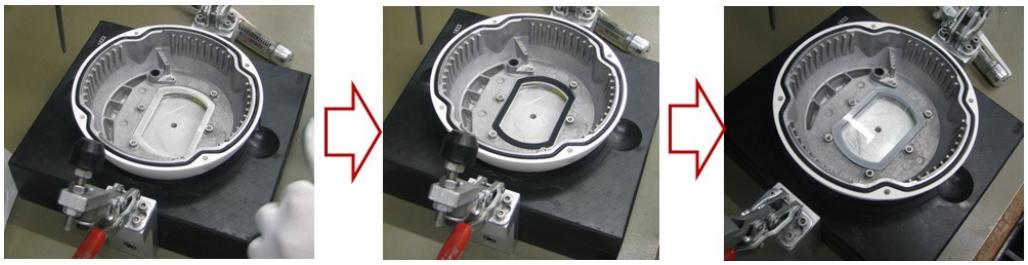

Figure 3.11: First part of the assembly

Afterwards the bezel is attached to the front shell with 6 screws, M4x8mm torx, which are tightened with a dynamometer tool with a torque of 0.4 Nm, having a tread locker adhesive applied to each one of them.

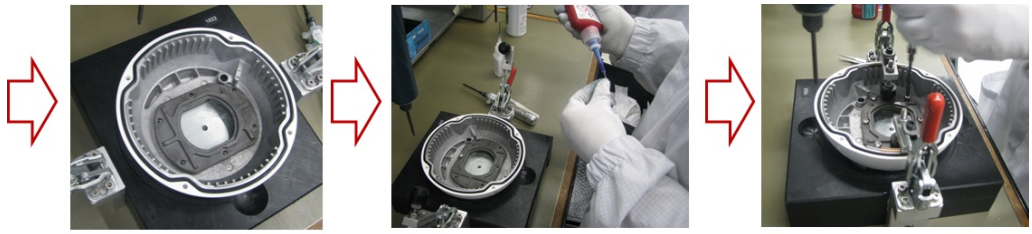

Figure 3.12: Second part of the assembly

Then a final torque of 1.8 Nm is applied to each screw according to the following pattern:

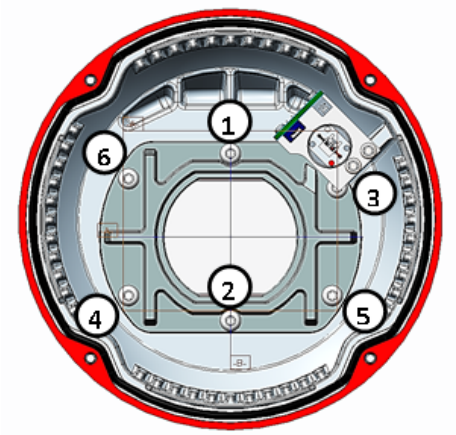

Figure 3.13: Tightening pattern

Once the bezel is fixed to the front shell, this last one is attached to the camera structure through 6 screws and then the camera is placed in a tank in order to proceed to the water tightness test, where it is submersed in water during 6 or 7 minutes.

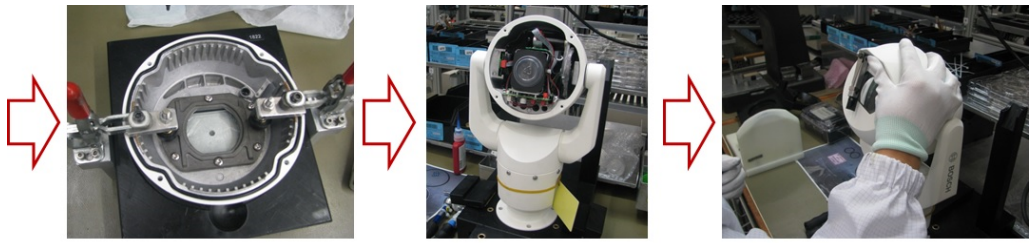

Figure 3.14: Third part of the assembly

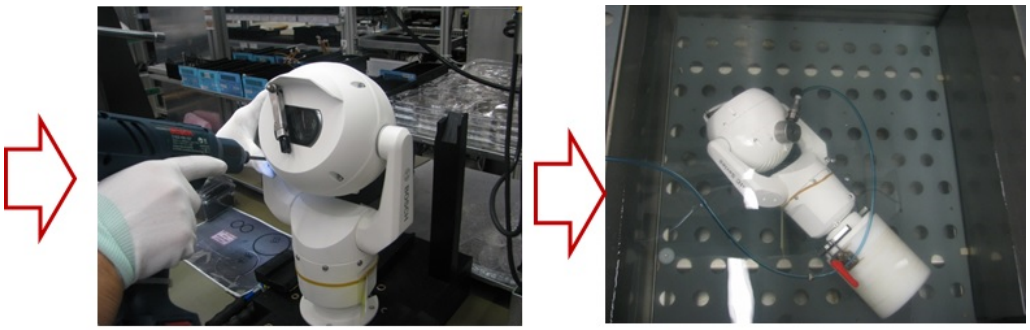

Figure 3.15: Forth part of the assembly

3.4 Primary analysis

In a first approach to the problem, Bosch tried to obtain the root causes of the window breakage by analyzing the different components and the assembly. In order to have a better understanding of the intervenient factors involved in this process, the critical dimensions were measured according to the corresponding tolerances. Regarding the front shell, problems related to dimension specifications were detected in April 2016, which lead PUQ to start controlling all these components. The dimensions measured were the flatness specification of the plane window, the flatness tolerance of the bosses, parallelism between the front shell face and the window, the bosses height and the parallelism tolerance, which does not take part in the drawing's specification, was also taken into account. Thus, it was verified if these dimensions were located between 0.05 and 0.1 mm.

The sighting led to conclude the flatness specification was verified as well as the height of the castles. However, the parallelism dimension was in the range mentioned above. Besides the possibility of having particles owing to the screw holes was analyzed, although it was not possible to obtain a conclusion on this matter.

Some glass window's dimensions were also examined, namely its thickness and the parallelism specified in the drawing. The first dimension was not confirmed since some values were out of specification and the second one was verified.

Both the glass window and the bezel are not controlled by PUQ after being received from the supplier. Concerning this last component, the controlled dimensions were its height, its flatness and the parallelism between the surface which touches the shell and the one touching the glass, which was also not defined in the drawing. The three dimensions were verified, concluding all of them were in the specification.

3.5 INEGI report analysis

This report is the result of an investigation carried out by INEGI in order to find the root causes for the window breakage, through the analysis of the different components and intervenient factors which could possibly contribute to the problem.

3.5.1 ESPI

When a rough surface is illuminated with coherent laser light (with only one wave length) and subsequently recorded with a CCD camera, statistical interference patterns are created – speckles. If a reference light is imposed to the speckles, the reflect beam and the reference beam are superposed, and therefore cause and interference pattern. When

the object is loaded and the surface deformed, the speckle interferogram changes and the comparison of the interferograms before and after loading results in a fringe pattern and consequently the displacement can be obtained.

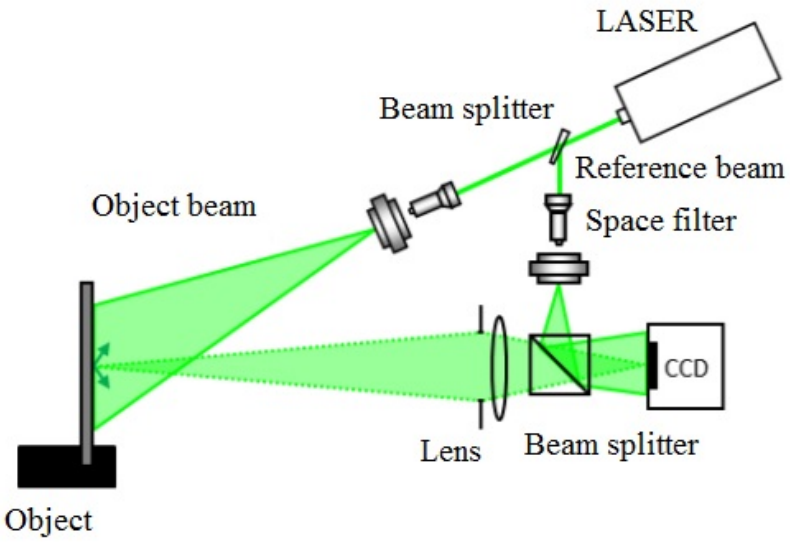

Figure 3.16: ESPI scheme

This technique was used as a validation of the numerical results provided by ABAQUS. In order to obtain this validation, 4 different front shells were analyzed using ESPI. Each one of them was placed in the JIG with the tight force used in Bosch and different values of pressure were applied: 0.02 bar, 0.04 bar and 0.06 bar. It was possible to verify not only the fringes resultant from the internal pressure applied in the display but also the stress concentration point on the bottom right corner, where the glass window preferably breaks.

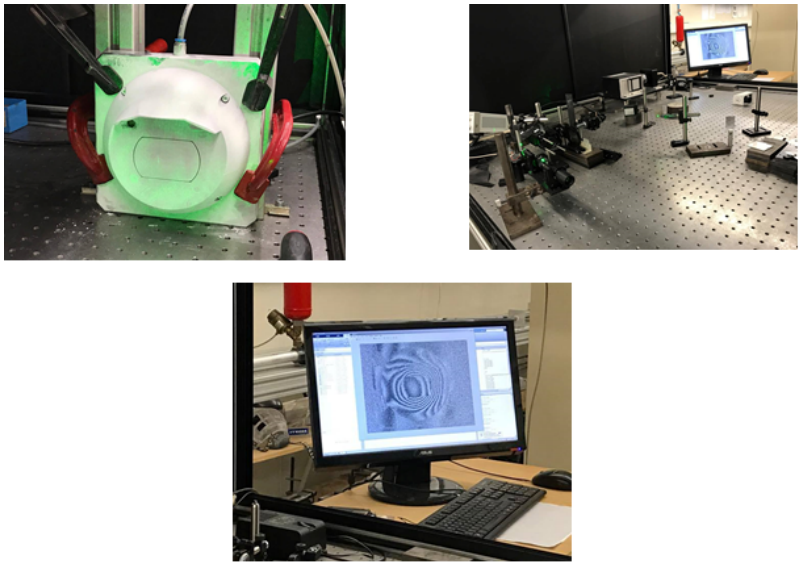

Figure 3.17: ESPI method applied on the front shell and on the glass window

The results among the different samples were very similar and the deformation for one of the shells is exhibited in figure 3.18, which corresponds to a pressure of 0.06 bar:

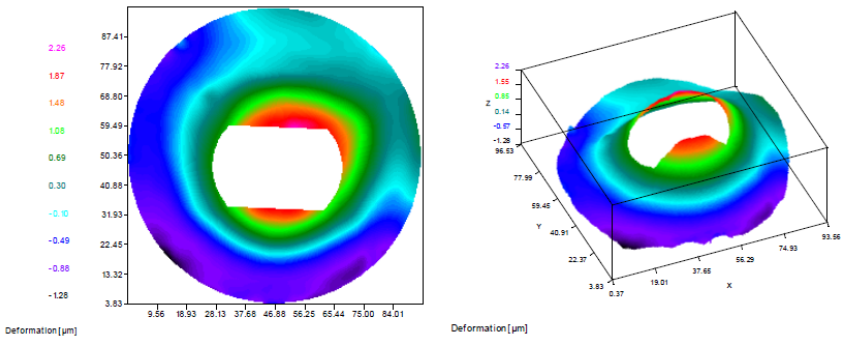

Figure 3.18: Deformation field for a front shell obtained through the ESPI method (0.06 bar)

It is possible to conclude the deformation is not symmetric, owing to the difference of stiffness, since on one side of this part there is a hole and a rib to attach and support the wiper and also due to the visor developed to protect the window from the rain, which grants more stiffness and therefore allows the glass window to twist, as it is presented in figure 3.19.

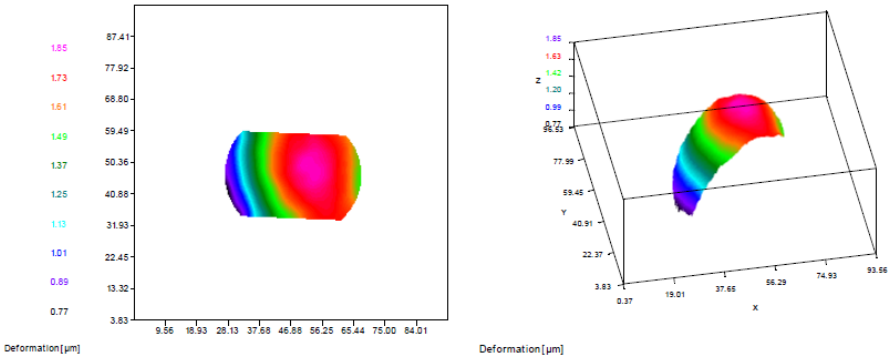

Figure 3.19: Deformation field for a glass window obtained through the ESPI method (0.06 bar)

3.5.2 Tightening torque

An analysis to the tightening torque was carried out to ensure the screws were attached with the recommended torque. In the following figure, it is possible to verify the measured values for the tightening torque from the factory, in red, and the values after tightening with the dynamometer from Bosch, in blue.

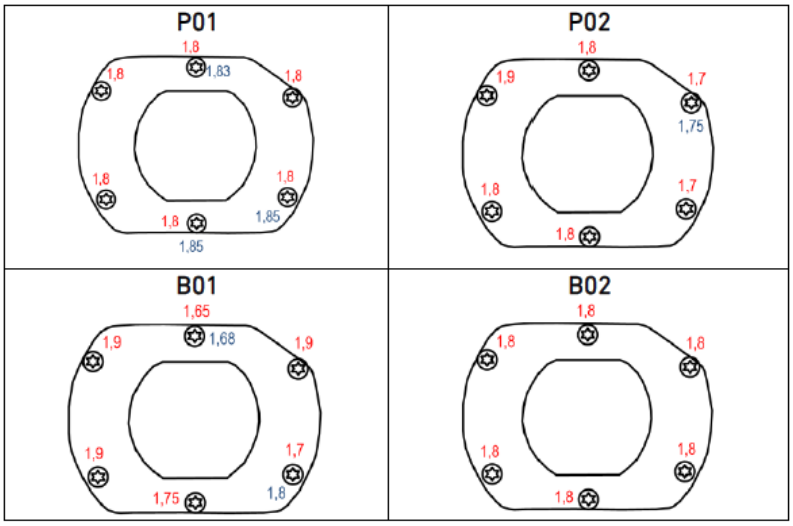

Figure 3.20: Measurement of the tightening force (Red: measured from the fabric; Blue: measured after tightening with Bosch's tool)

3.5.3 New gasket

The replacement of the old gasket model for a new model is a possibility Bosch has been considered and therefore the company already had a gasket prepared to be tested. Thus, a new ESPI test was implemented and the gasket was replaced with a similar one, with the main aim of concluding if the displacement and stress fields would be more uniform. Considering a pressure of 0.04 bar, the front shell and the glass window presented the following behavior:

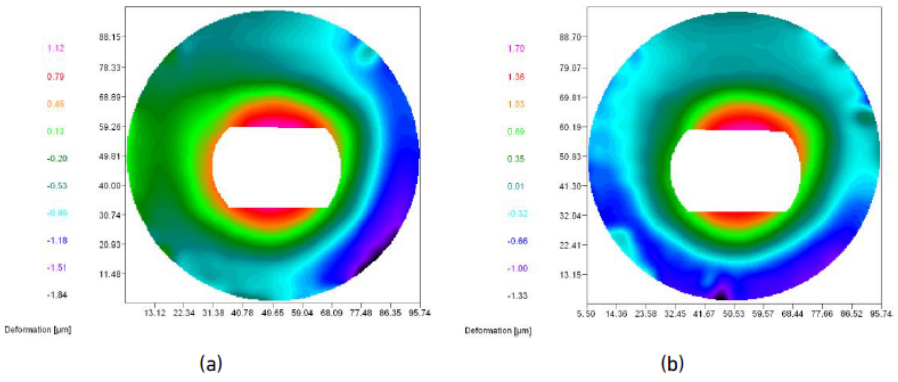

Figure 3.21: Deformation field considering the old (a) and the new (b) gasket obtained through the ESPI method for the front shell

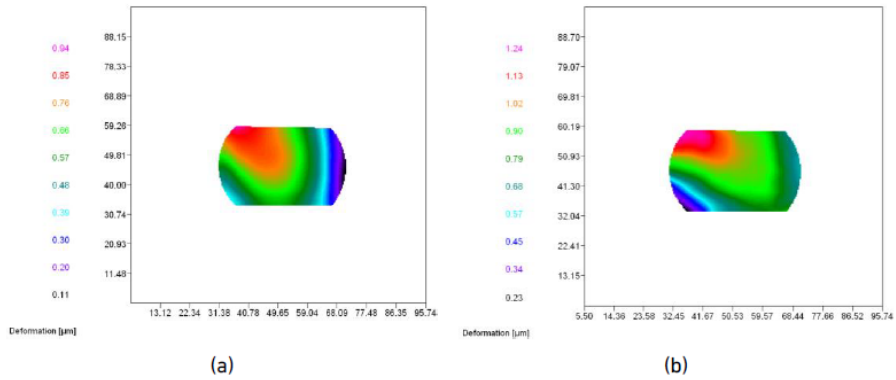

Figure 3.22: Deformation field considering the old (a) and the new (b) gasket obtained through the ESPI method for the glass window

Through the analysis of figures 3.21 and 3.22 it is possible to verify the deformation values are higher for the new gasket case.

A comparison between the old gasket and the new one also took place based on a compression test, using a universal test machine, exhibited in figure 3.23. This test consisted of 3 compression loadings of 1.5 mm with a velocity of 0.1 mm/s in 3 different random points.

Figure 3.23: Compression test

In figure 3.24 the comparison between the loadings and displacements for both the gaskets is exhibited:

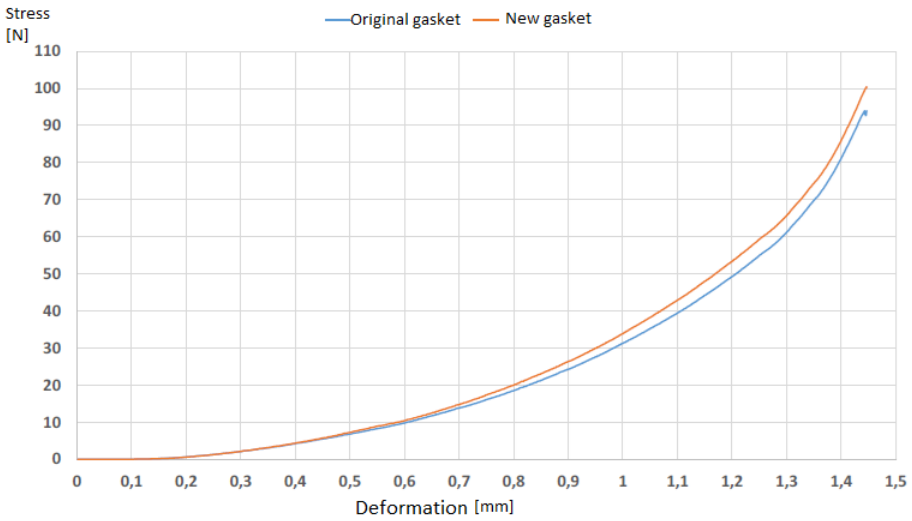

Figure 3.24: Comparison between the loadings and displacements for both the gaskets

Since the compression the gasket is subjected to is about 0.77 mm, it is possible to conclude the difference between the loading of these components is about 2 KN.

3.5.4 Photoelasticity

This method consists of measuring the strain state or stress state of a component based on a characteristic – birrefringence - of some transparent materials, whose optical behavior is dependent on the stress or strain they are subjected to.

The glass windows were exposed to a polariscope and despite of its low birefringence, it was possible to verify the residual stress concentration points on each corner through the variation in the distribution of light intensity, owing to the strengthening process. As an example, an intact window is presented in figure 3.25:

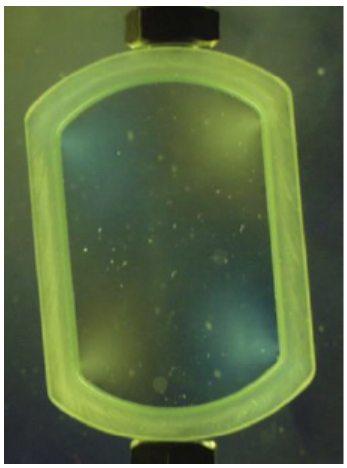

Figure 3.25: Residual stress concentration in a glass window observed through the polariscope

3.5.5 Fracture analysis

From the analysis of the fracture surfaces, it was possible to identify the crack's origin: it started in the internal polished surface and propagated towards the machined surface. It was also possible to distinguish the presence of some external particles crushed towards the gasket which could possibly contribute to failure. This fact led to carefully analyze the front shell in order to identify the particles and their origin.

Most of the particles found in the front shell seemed to be polymeric, despite of some evidence of the presence of metallic particles as well. On the top of the bosses and on the lower flat surface of the front shell, the particles seem to belong to Loctite.

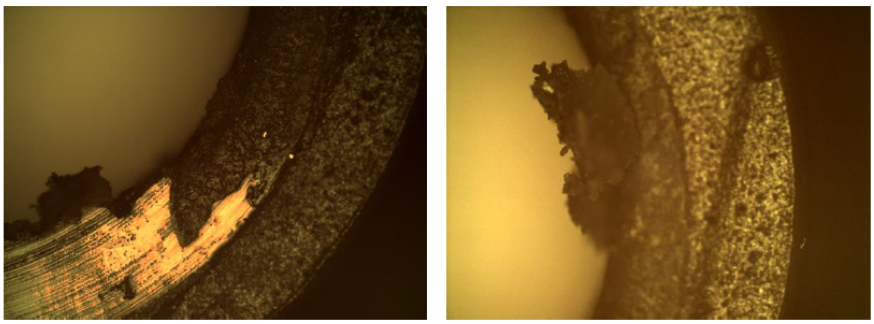

Figure 3.26: Particles found on the bosses

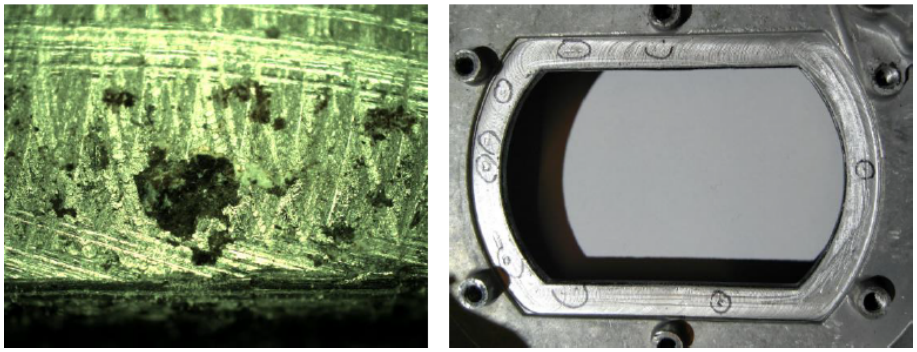

Figure 3.27: Particles found on the shell

3.5.6 Proposed solution

Since the glass window breakage is not a recurrent occurrence, the root causes of this issue are probably related to geometrical variation of the cavity where the window is placed. Thus, it is possible to simulate loadings resultant from the external conditions the camera it subjected to: temperature and pressure variation. The former case is related to the solar exposition and the day/night cycle, while the latter is associated with the thermal differential between internal and external areas and the watertightness required for the front shell. Besides, the electric circuits also generate heat. Therefore, a numerical model in ABAQUS was used so the different service conditions could be simulated and consequently analyzed.

The mechanical properties considered for the different materials are presented in the following table:

Table 3.6: Mechanical properties used in the numerical simulations

Material	Poisson's ratio	Young Modulus (MPa)	Density (kg/m^3)
Aluminum	0.26	70 000	2700
Polyurethane	0.48	25	1200
Glass	0.23	65 000	2500

The results for a front shell whose applied stress was 0.06 bar is exhibited in figure 3.28:

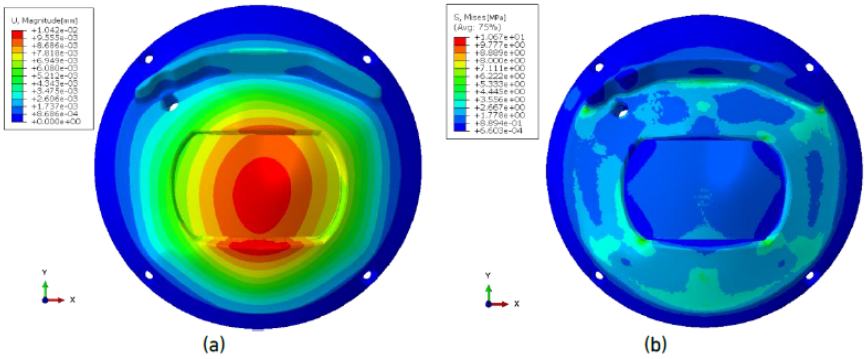

Figure 3.28: Deformation and strain for the camera considering a pressure of 0.06 bar

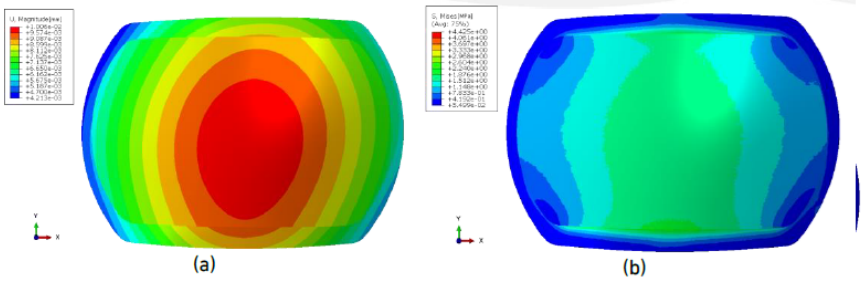

Figure 3.29: Deformation and strain for the glass window considering a pressure of 0.06 bar

Since the front shell is not a symmetric component, as already mentioned and justified above, the proposed solution by INEGI consists of reducing this asymmetry by adding a rib on the bottom of the internal side of the shell. This modification would not imply large costs but only a small change in the injection mold.

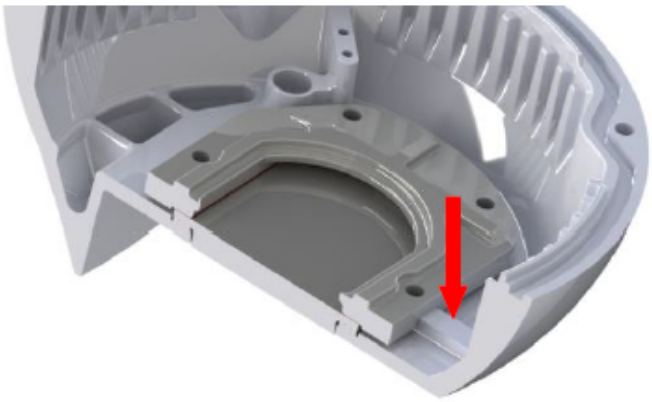

Figure 3.30: Proposed solution by INEGI: rib

The numerical model was used to determine the displacements and stress resultant from the addition of the rib to the front shell. As it can be seen in figure 3.31, the deformation distribution is in this case more uniform and in figure 3.32 it is possible to verify the deformation field is less aggravated in the corners, comparing to figure 3.29.

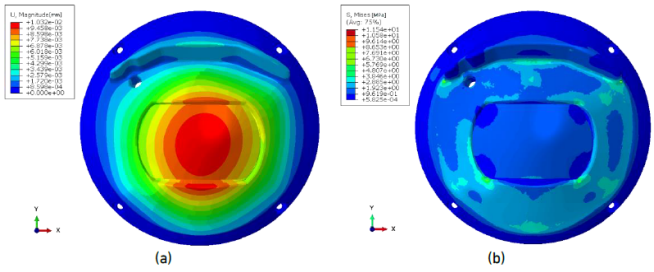

Figure 3.31: Proposed solution by INEGI: rib

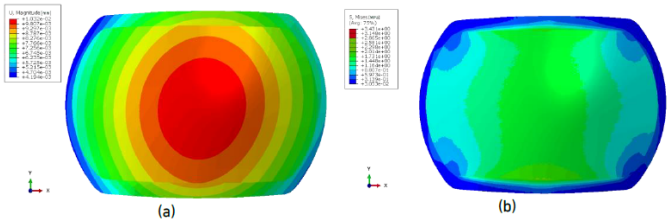

Figure 3.32: Proposed solution by INEGI: rib

3.5.7 Metrology

The system watertightness is ensured by the compression between the bezel, mylar, glass window and gasket through the controlled tightening of the screws and every surface should have an appropriate tolerance to guarantee a uniform stress distribution created by the screws' tightening.

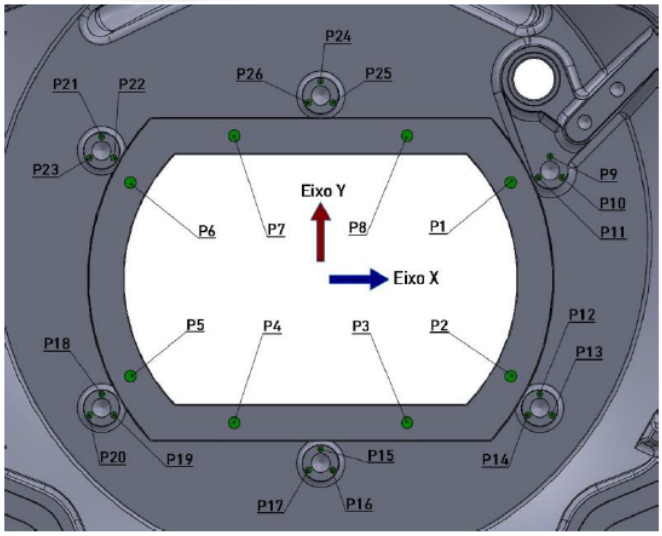

Figure 3.33: Points considered fot the metrologic analysis

Thus, a metrologic analysis to the surfaces of the 3 front shells (P02, B02 and A1) which are in contact with the gasket was made, in order to obtain their real dimensions, as well as the boss's height. In each front shell, 26 points were measured, 8 in the lower surface of the shell and the remaining in the bosses, as it is presented in figure 3.33.

The results for the deviation in each point for each sample, concerning the first 8 points associated with the lower surface which is in contact with the gasket are presented below:

Table 3.7: Minimum and maximum height and deviation for the machined surface of the front shell considering 3 cameras: P02, B02 and A1

Material	Minimum Height [mm]	Maximum height [mm	Deviation ([mm]
P02	2.716	2.863	-0.147
B02	2.667	2.909	-0.242
A1	2.688	2.783	-0.095

The deviation with respect to this machined surface is between 0.095 mm and 0.242 mm, while the flatness specification is defined as 0.1 mm.

Regarding the remaining 26 points, the results are presented in the following table and chart:

Although the dimensional tolerance associated with the boss's height is 5.2 $\pm$ 0.1 mm, the deviation is between 0.116 and 0.322 mm.

3.5.8 Conclusions

There were no conclusive results about the root causes for the window breakage, despite of the presence of some factors combined together which can justify this problem. In order to obtain a correct identification of the cause, it would be necessary to run a systematic analysis of the process in a longer period time, collecting several samples corresponding to different periods of production of the different components.

The ESPI analysis allows to conclude the front shell's deformation is not uniform leading to a non-uniform displacement of the glass window. Besides, the presence of residual stress concentration, a variation in the tightening force and a dimensional variation in the boss's height may also contribute to failure.

In addition, the presence of small particles, metallic and non-metallic, in the glass surface combined with the fracture surface analysis lead to conclude the crashing of these particles between the gasket and the machined surface may cause the fracture origin, since the fracture seems to initiate in the opposed surface, which is in tension and whose yield strength is inferior than the one from the surface subjected to compression.

Since all the tested windows presented particles, the production process should be strictly controlled in order to avoid other problems related to the requirement of watertightness.

The numerical model confirmed the proposed solution, which consists of adding a rib to the front shell, would present more uniform stress distribution values.

3.6 Analysis of samples

Bosch's glass supplier provided some samples of the glass window in the different stages of production: float glass without any strengthening, machined glass and then chemically strengthened glass. These samples were placed in the polariscope in FEUP in order to determine in which phase the residual stress concentration visualized in the corners appeared. In figure 3.34 it is represented a glass window which has not been strengthened but has been machined and in figure 3.35 there is chemically strengthened and therefore it is possible to conclude the residual stresses are resultant from the strengthening process, since the samples from this stage are the ones who present fringes in the corners.

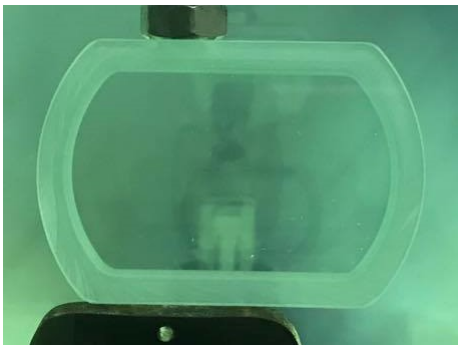

Figure 3.34: Glass window before the chemical strengthening exposed to a transmission polariscope

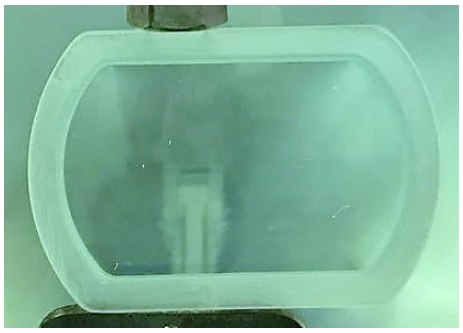

Figure 3.35: Glass window after the chemical strengthening exposed to a transmission polariscope

3.6.1 Case depth determination

Regarding the chemical strengthening process applied to the glass, which consists of exchanging Na^+ ions for K^+ ions provided by the molten salt bath, the exchange layer is thin, even with a specification of 30-50 μm, since the supplier cannot ensure this thickness because he is not able to measure it. According to Glaesemann, a SLS glass does not have a compressive stress layer thicker than 15 μm while there are other types of glasses whose ion exchange layer can reach 50 μm. This fact is due to the high temperatures below the transition point which induce stress relaxation, implying diffusion effects in common glasses. Soda lime glass products are slow to develop a 25 μm case depth even if immersed for 4-24h [11].

These facts led to a suspicion of having a glass window whose case depth was not only out of the specification but probably also presented a very low case depth. In order to confirm this type of glass was not respecting the drawing specifications, a chemical was carried out in CEMUP (Centro de Materiais da Universidade do Porto), a centre of materials, with the main aim of measuring the thickness of the compressive stress layer resultant from the chemical strengthening. In CEMUP, a SEM (scanning electron microscope) used a focused beam of high-energy electrons to generate a variety of signals at the surface of solid specimens, which provided information about the chemical composition.

In a first analysis, a sample of the broken glass was analyzed in 4 different areas, represented in figure 3.36:

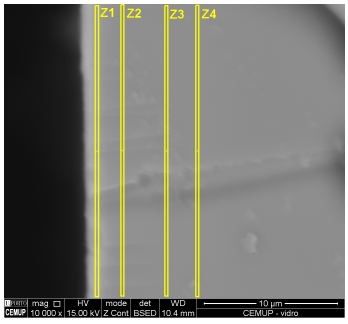

Figure 3.36: Analyzed areas of the glass sample

The chemical composition for the different areas are presented in figures 3.37 and 3.38:

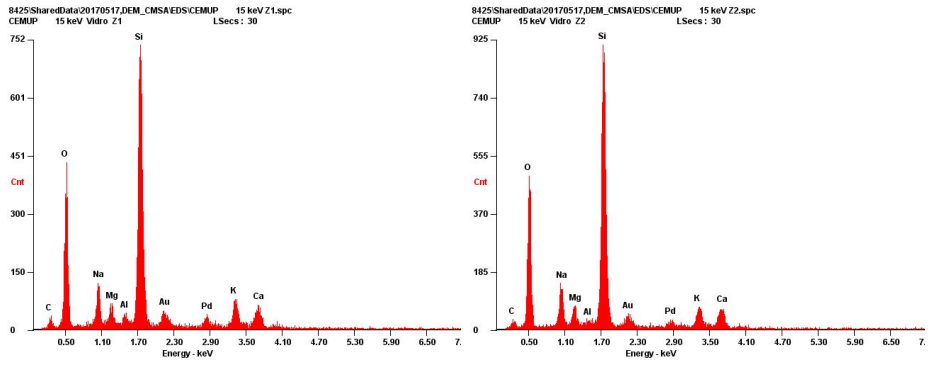

(a) Chemical composition for z1 (b) Chemical composition for z2

Figure 3.37: Chemical composition for the first two regions of the sample

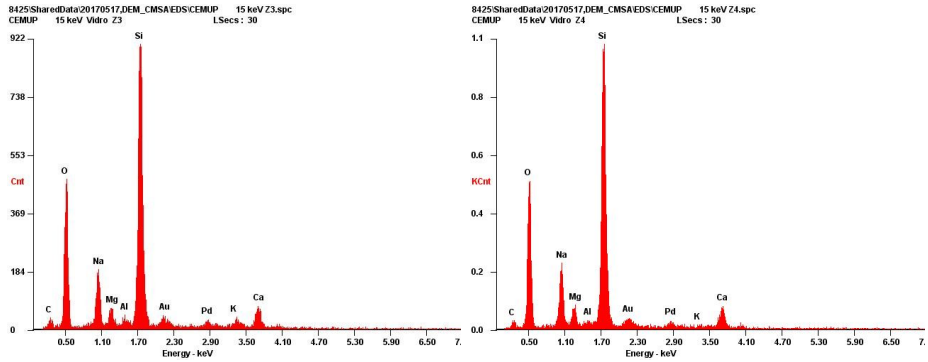

(a) Chemical composition for z3 (b) Chemical composition for z4

Figure 3.38: Chemical composition for the last two regions of the sample

By analyzing the charts exhibited in figures 3.37 and 3.38 it is possible to verify the potassium concentration is significantly higher in areas z1 and z2, while it decreases in z3 and z4, leading to conclude the layer of compressive stress reaches z3 but with a lower amount of potassium, and in z4 there is almost no potassium and therefore the layer is practically nonexistent. The concentration of each constituent is presented in figure 3.39, where it is possible to confirm the concentration of potassium corresponds to a zone whose thickness is between 3 and 4 μm.

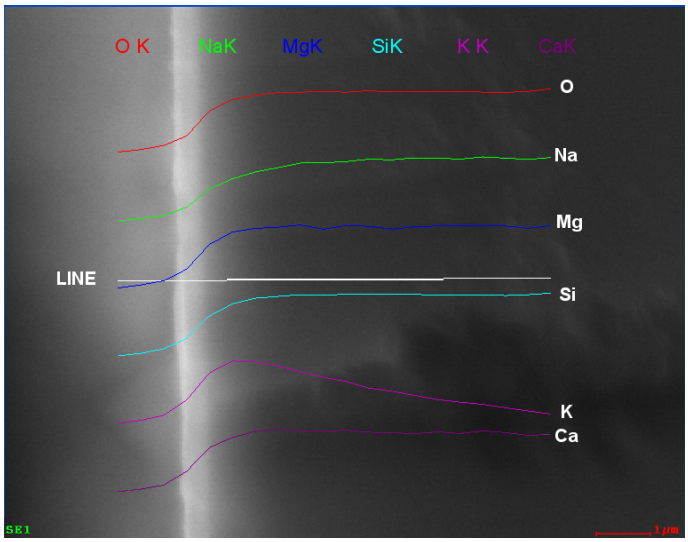

Figure 3.39: Concentration of the constituents along the glass thickness

Since the first sample was not well prepared and in the best conditions to be analyzed, a second analysis was carried out using another sample where three regions were analyzed: L2, L3 and L4, presented in figures 3.40, 3.41 and 3.42:

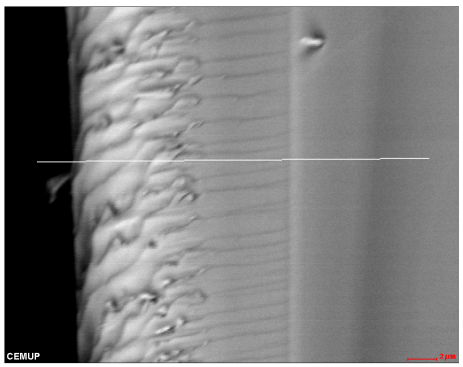

Figure 3.40: Reference line from region L2 which contains the analyzed points

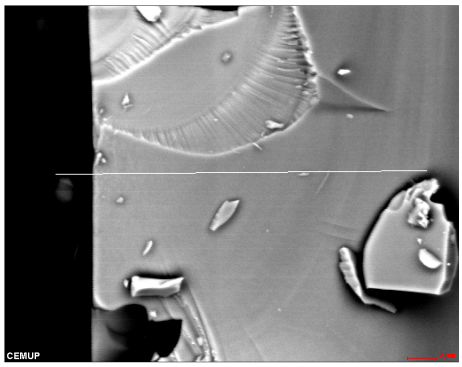

Figure 3.41: Reference line from region L3 which contains the analyzed points

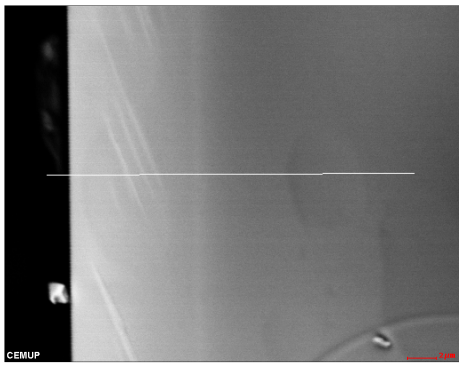

Figure 3.42: Reference line from region L4 which contains the analyzed points

Each line was analyzed in 4 different points: on the border (at 1 μm from it) and at a 10, 15 and 20 μm from it, as it is presented in figure 3.43:

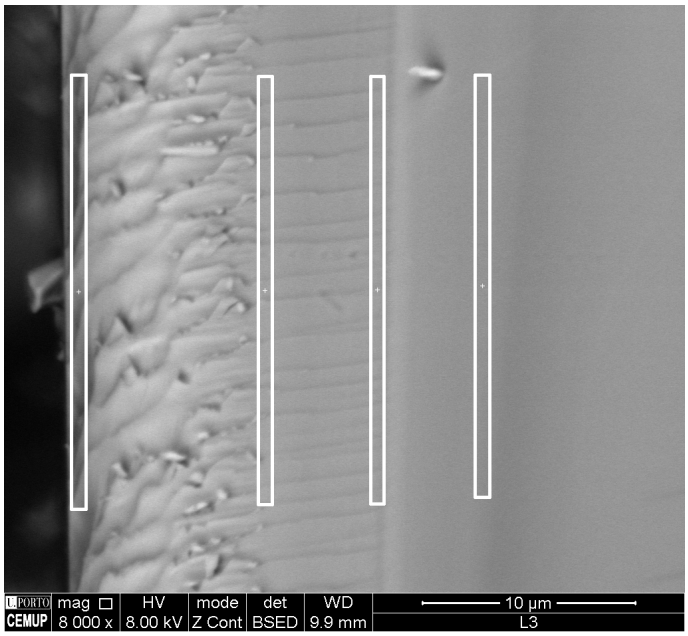

Figure 3.43: Regions where L2, L3 and L4 were analized

Regarding L2, the results for the 4 points analized are presented in figure 3.44, and 3.45:

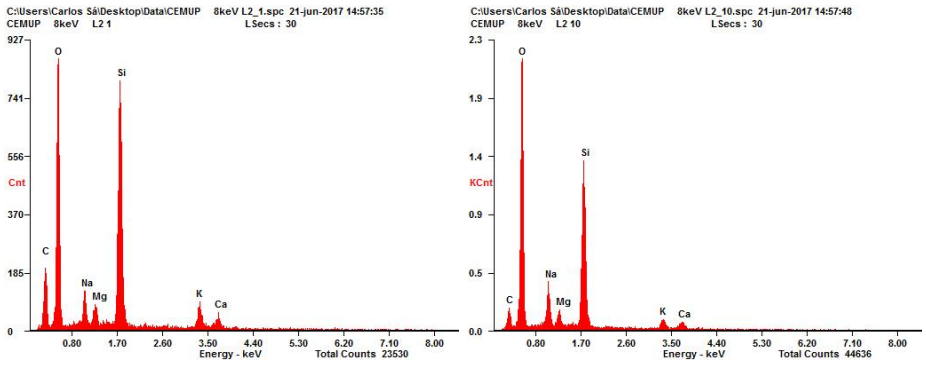

(a) Chemical composition for 1 μm (b) Chemical composition for 10 μm

Figure 3.44: Chemical composition for the two first points of L2

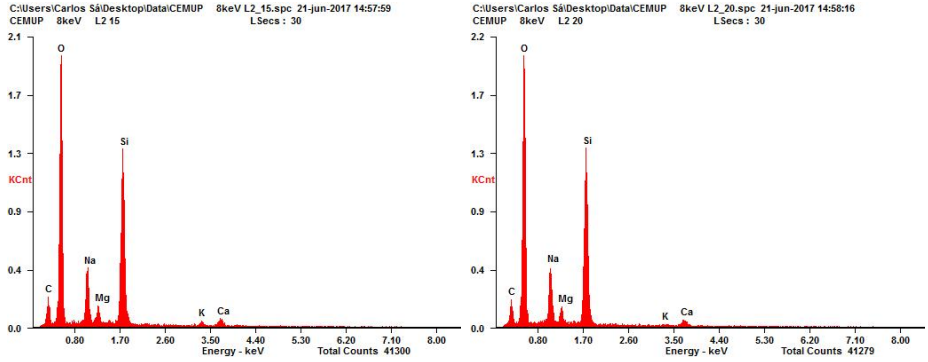

(a) Chemical composition for 15 μm (b) Chemical composition for 20 μm

Figure 3.45: Chemical composition for the two last points of L2

The percentage of potassium from the border of the sample in L2 to the interior can be seen in table 3.8, and it is possible to conclude at 20 μm the concentration of it is pratically non-existent.

Table 3.8: Percentage of K from the border to the interior of L2

Points	K (Wt %)
1 μm	13.6
10 μm	8
15 μm	3.6
20 μm	1.6

With regard to L3, the results for the 4 points analized are presented in figure 3.46 and 3.47:

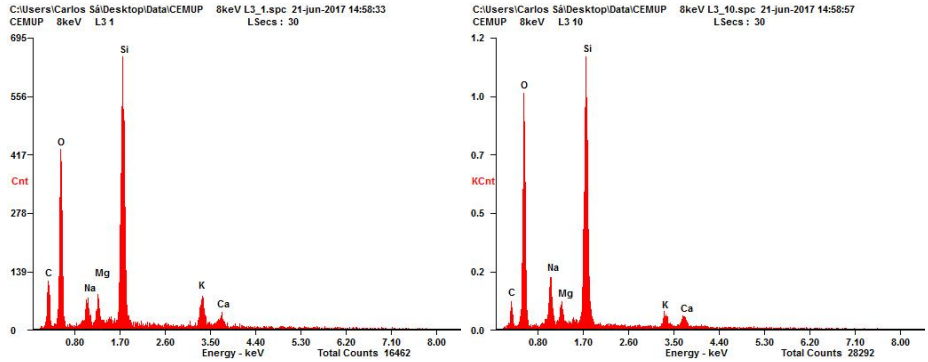

(a) Chemical composition for 1 μm (b) Chemical composition for 10 μm

Figure 3.46: Chemical composition for the two first points of L3

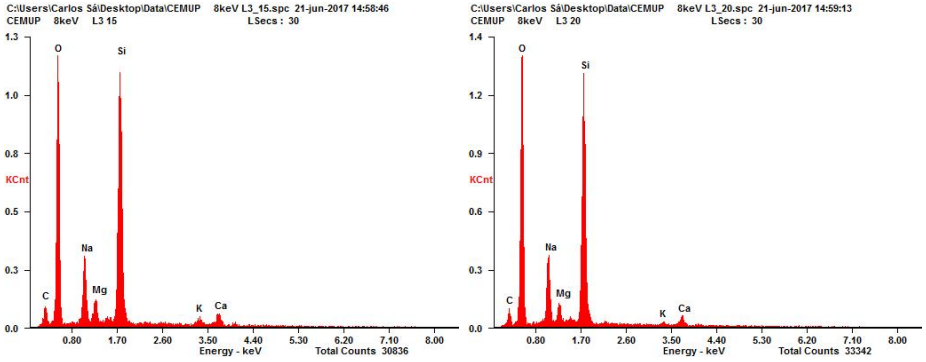

(a) Chemical composition for 15 μm (b) Chemical composition for 20 μm

Figure 3.47: Chemical composition for the two last points of L3

Since the percentage of potassium at 20 μm is 2.2, as it can be seen in table 3.9, it is possible to conclude it is also pratically non-existent.

Table 3.9: Percentage of K from the border to the interior of L3

Points	K (Wt %)
1 μm	15.6
10 μm	8.1
15 μm	4.6
20 μm	2.2

The results for the 4 points analized in L4 are presented in figure 3.48 and 3.49:

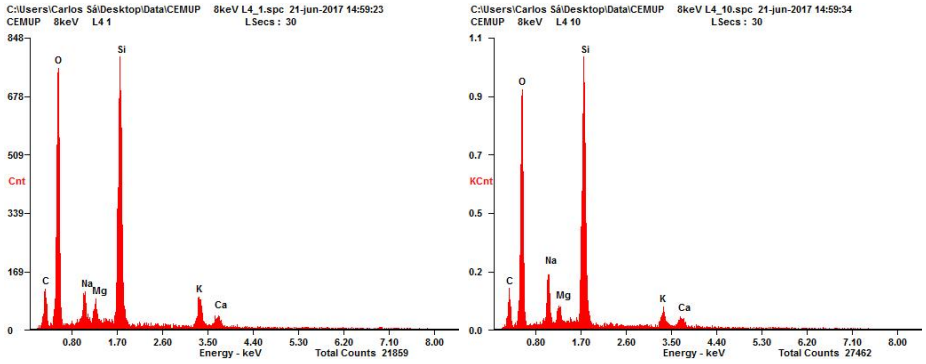

(a) Chemical composition for 1 μm (b) Chemical composition for 10 μm

Figure 3.48: Chemical composition for the two first points of L4

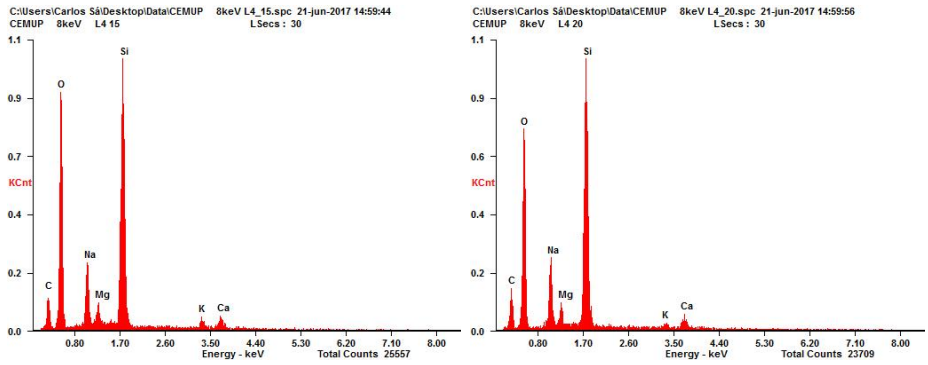

(a) Chemical composition for 15 μm (b) Chemical composition for 20 μm

Figure 3.49: Chemical composition for the two last points of L4

Once again the percentage of potassium at 20 μm is very low, 2.4, presented in table 3.10, and thus considered non-existent.

Table 3.10: Percentage of K from the border to the interior of L4

Points	K (Wt %)
1 μm	14.5
10 μm	8.5
15 μm	4.8
20 μm	2.4

Through the evaluation of the previous results where the concentration of potassium is out of specification, which should be between 30 and 50 μm, it is possible to confirm the suspicion about the efficiency of this process in a soda-lime glass.

Chapter 4

Proposed solutions

The solutions here proposed are based on the study and analysis concerning the different components and factors which may interfere in the glass window breakage and therefore the critical issues were examined in order to adjust some of them and project some modifications so the breakage can be prevented.

The main root causes provided by the INEGI report were considered and consequently the solutions will be directly related to them.

4.1 Glass

The previous analysis concerning the glass window production and chemical treatment led to a more intense study regarding these subjects. The chemical strengthening process was reviewed in order to conclude not only if it is possible to find a more suitable strengthening process or to replace the SLS glass with an equivalent one, stronger and cost-effective, or even with a polymer. Besides, the glass geometry will also be considered and modified so the stress concentration point is removed and the difference between the shell deformation and the glass window deformation is eliminated or at least smoothed.

4.1.1 Glass type

SLS is the most commonly used glass since 90% of all glass manufactured globally has this composition, even if containing other minor constituents. This type of glass contains about 74% of silica, which implies a high cost owing to high temperature, leading to the addition of soda, in order to decrease the temperature required for melting. However, a large amount of soda may also involve poor chemical durability, and therefore a small portion of the soda is replaced with lime, so it offsets the reduction in chemical durability also with a reasonable melting temperature [6].

The main advantage of chemical strengthening is the applicability to thin glasses, whose thickness is even lower than 1 mm, and glasses with complex shapes. Moreover, the strength value becomes two to five times greater [17]. In some industrial glasses, it is not possible to avoid damage during processing or handling before the chemically strengthening process, and such damage has an impact in the strength of the ion exchanged glass, even when an etching process is performed before the strengthening. Therefore, a comparison between other glasses is here presented so it is possible to analyze the hypothesis of replacing the SLS for another type of glass. It is also important to only consider glasses which can be subjected to the ion exchange process, meaning only alkali-containing glasses.

Alkali aluminosilicate glasses

According to Varshneya, with a soda-lime-silicate glass it is possible to get a good strengthening with about 25 μm case depth and a compressive stress from 400 MPa to 700 MPa. However, it is also possible to improve these values by using other types of glass, for instance, alkali-aluminosilicate glasses, in which the strengthening is considered very good.

Thus, other type of glasses such as aluminosilicate (ALS) were developed in order to replace SLS, since alkali metal diffusion is faster in ALS and viscous relaxation at treatment temperature is slower, leading do higher surface compression and larger case depth levels, giving rise to a high internal tension [11].

The presence of non-bridging oxygen, consisting of relatively weak places in the glass structure, which leads to a high "densification" of the glass structure after the ion exchange process and thus, a relatively low value of the stress built up [19]. The extent of the relaxation of the stresses are mostly influenced by the viscosity of the high-density structure, which in some glasses is related to the viscosity of the non-ion-exchanged glass. In alkali-aluminosilicate glasses the introduction of Al_2O_3 increases the rigidity of the network due to the removal of non-bridging oxygen ions and therefore these glasses are well suited for reinforcement by the building up of compressive stresses [19].

ALS typically contain 10 to 25% of Al_2O_3 while the alkali content is over 10% and this high alkali content prepares the glass for ion exchange, with larger alkali ions, and consequently the surface compressive strength is improved. It has high transformation temperatures and outstanding mechanical properties, such as hardness and scratch behavior.

Aluminosilicate glasses are commercially used for several glass products, such as cover glass applications [37] and halogen-lamp glass.

The flaws present at a glass surface can be resultant either from a force acting on the surface being more or less parallel - a situation where scratches are produced – or from a force acting on the surface more or less normal to it, where craters are produced and found in impact experiments or when a glass object is dropped on the ground. The scratches resultant from the former case have an estimated depth between 20 and 30 μm while latter leads to craters with 10-20 μm and cracks which extend from them through the glass to a depth of 40-60 μm and thus the compressive stress layer must have at least 60 μm [19].

Aluminoborosilicate glasses

ALBS glasses usually contain 55 to 65% of SiO_2, 15–20% Al_2O_3, 5–10% B_2O_3 and about 10 to 15% alkaline earth oxides, without the presence of alkali oxides. A low coefficient of thermal expansion combined with high transformation temperature and good chemical stabilities are good characteristics of this glass type which make it particularly useful as substrate glasses for flat panel displays. ALBS glass satisfies not only the high crack resistance requirement but also effective chemical strengthening.

Morozumi compared an SLS glass with two ALS and one ALBS in terms of the thickness of the compressive layer and on the crack formation probability before chemical strengthening. The depth of this layer was larger for the ALBS glass and lower for the SLS. In addition, the ALBS showed the lowest crack formation probability before stengthening, concluding it would be well suited for safety cover glass [17].

4.1.2 Strengthening

Since the most competitive strengthening process is thermal tempering, a brief and explicit comparison between chemical strengthening and thermal tempering is presented:

Table 4.1: Comparison between chemical strengthening and thermal tempering

Chemical Strengthening	Thermal Tempering
Pros	**Pros**
Very high surface compression - 1000 MPa;	Extremely tough outer surface;
Almost no geometric distortion;	
Small internal tension;	
Complex geometries;	High pressure applications.
High-performance applications;	
It can be performed in thinner glass,	
with sections <2 mm thick	
Cons	**Cons**
Low case-depth for SLS	A minimum thickness of 3 mm is required;
Cost expensive;	Not resistant to temperature changes;
Several hours of immersion process;	Shatters under extreme temperature stress;
Several hours of immersion process;	Lower maximum strength;
Any efforts to get profiles deeper than	
35 μm in SLS glasses result in relaxed	
stress profiles	It has a high coefficient of expansion;
Cost expensive;	
Several hours of immersion process;	The edges are the weak point.
Several hours of immersion process;	

The mechanism of ion-exchange depends on the diffusivity of the respective ions, and the highest diffusivities are generally found for aluminosilicate compositions. These glasses provide the most useful materials by yielding compressive layers of practical thicknesses in realistic treatment times [22] and according to Varshneya chemical strengthening technology works best for lithium and sodium aluminosilicate glasses. Regarding common soda lime silicate glass, chemical strengthening is generally not very suitable since any efforts to increase the case depth lead to the relaxation of surface compression [13].

A KNO_3 bath is usually used for a glass containing sodium while a $NaNO_3$ is generally used for a lithium-containing glass. As mentioned above, since the stress production strongly depends on the interdiffusion coefficient of the alkili ions with the salt ions and therefore the glass composition should have a high concentration of mobile ions. Besides, since relaxation phenomena is activated by temperature and stress, higher exchange temperatures lead to higher relaxation rates [38].

Improving the chemical strengthening process may be a good measure to be implemented since with a two-step ion exchange it would be easier to get a larger case depth. This method consists of adding, for instance, lithium to the glass and immerse it in a Na-K

mixed molten salt bath and then again in a potassium nitrate bath (KNO_3). The first exchange will be between the Li^+ ions and the Na^+ and K^+ ions and later the Na^+ ions will be replaced with K^+ ions, ensuring a deeper layer of compressive stress [17]. However, although multistep strengthening technology, such as the two-step ion exchange mentioned above, has been tried, they are generally of limited use. The possibility of performing a multi-step ion exchange comes with the fact that a significantly deeper compressive layer can result from a first step where smaller ions at high temperature can penetrate deeply into the glass and followed by a subsequent exchange with larger ions, when comparing with a single-step process [11].

The best chemical strengthening process which can be achieved in a single-step strengthening process was demonstrated by Varshneya for a high T_g using a lithium aluminosilicate glass immersed in mixed $NaNO_3/KNO_3$ baths attaining a surface compression of approximately 1 GPa, decreasing rapidly to about 280 MPa at around 40 μm, then slowly decreasing to zero at 1 μm depth [11].

4.1.3 Geometry

Regarding the glass geometry, the most obvious aspect to be analyzed is the presence of the corners in the glass window and therefore the creation of new geometries considering this matter is an important modification whose main aim is to reduce the residual stress concentration present in these areas with the polariscope, as it can be seen in figure 4.1. The cameras with the new geometries were later tested based on the finite elements method in order to verify if the changes would solve this problem.

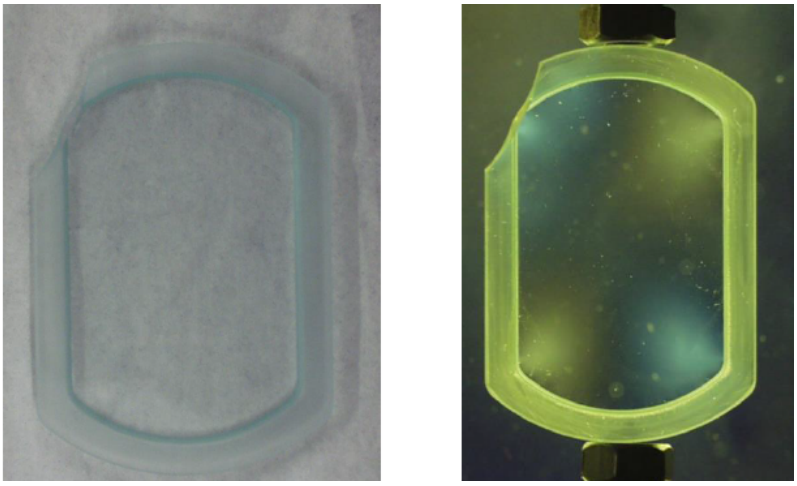

Figure 4.1: Residual stress areas to be eliminated with the modification of the glass window geometry

Since this action will not only change the glass window geometry but also the geometry of the bezel and front shell, there most relevant requirements to be considered is the field of view, which has a rectangular shape with a length of 44.55 mm. The glass window's thickness was not modified in any of the solutions presented below.

Circular

A circular glass window was the first hypothesis since there should be no possible stress concentration features considering this shape, despite Bosch has been maintaining the glass geometry through all the new MIC products and so adding such a radical change was seen as "aesthetically unacceptable". Nonetheless, in order to verify if this geometry would be the ideal one, a circular glass window was attained, as it can be seen in the following figures, containing all the components.

The field of view is integrated in a circumference with a diameter of 44.55 mm and so the diameter for the glass window must be at least equal to this value. Therefore a diameter of 48 mm was chosen, both for the glass window and for the other components such as the front shell, the insulator and the gasket.

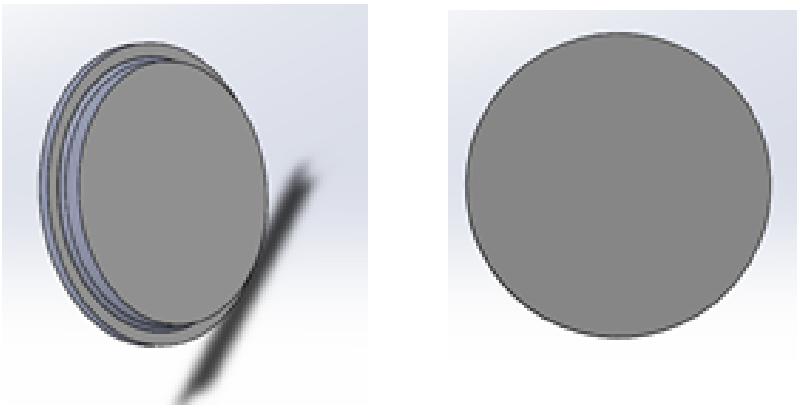

Figure 4.2: Glass window with a circular shape

Besides the cavity shape, there was another alteration in the front shell: the number of screws was reduced from 6 to 4 and therefore only 4 bosses were considered for this solution.

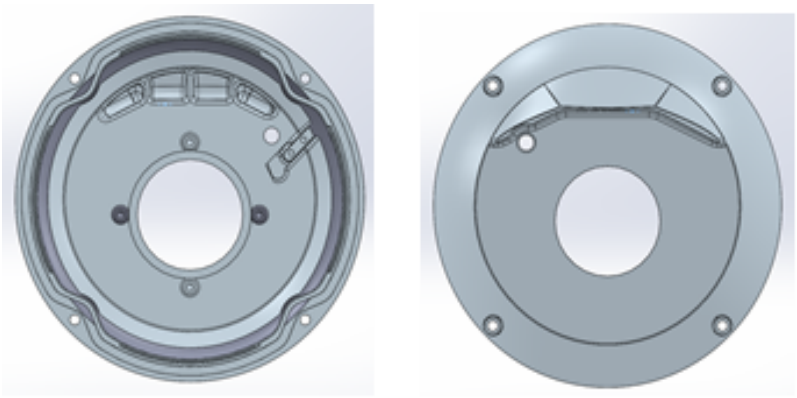

Figure 4.3: Front shell with a circular shape for the glass window

The bezel was the component which suffered more changes since its shape was adapted to circle and instead of having 6 holes for the screws, only 4 holes were integrated in this component. This modification from 6 to 4 screws might affect the water tightness and thus this solution would require tests regarding the new torque applied in order to ensure the gasket would continue to be compressed. The glass's exterior diameter, which means the diameter of the machined face is 55 mm, and consequently the bezel's interior diameter

presents the same value.

Figure 4.4: Bezel with a circular shape for the glass window

Both the insulator and the gasket present a circular shape and the latter maintains the near-2-cylinder transversal section.

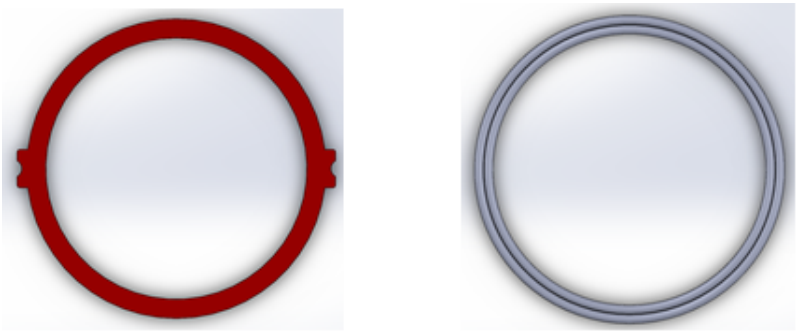

Figure 4.5: Insulator and gasket with a circular shapes

The assembly of the different components is presented in figure 4.6:

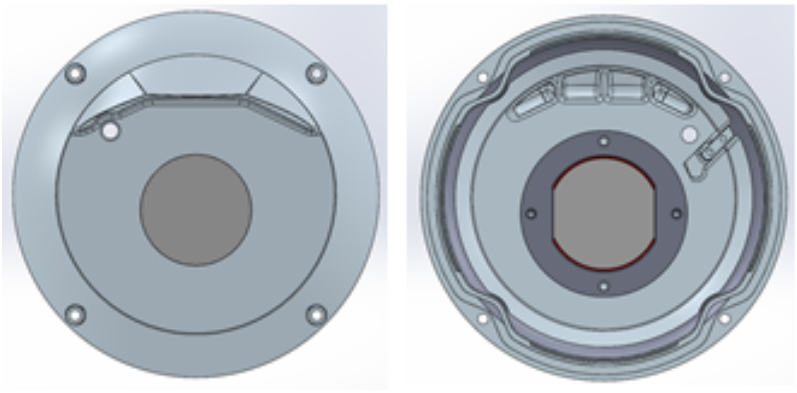

Figure 4.6: Assembly of the components with a circular shape

Looking at the front-shell geometry would result in concluding this component continues asymmetrical and thus a rib (initially suggested by INEGI) was introduced inside the shell in order to compensate the rigidity effect provided by the rib of the wiper engine.

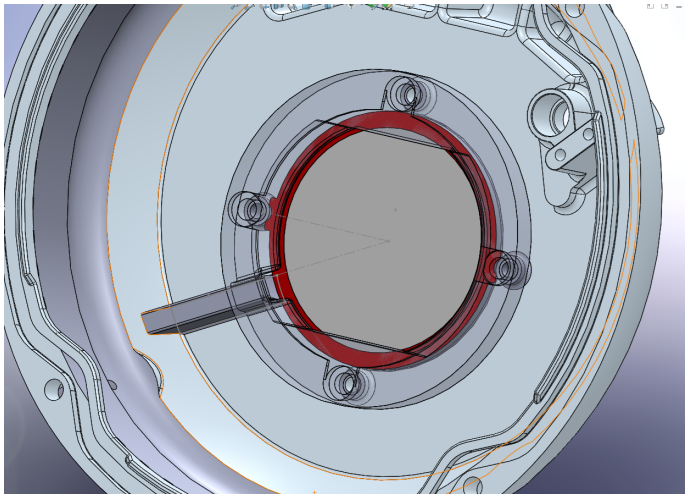

Figure 4.7: Camera with a circular shape and a rib

Rounded corners

The main aim of this second change is trying to eliminate the corners and approximate its shape to a circle. The geometry suggested maintains the x- direction in order not only to ensure it does not affect the field of view and also because another goal is making the minimum possible changes in the other components as well. The new dimensions of this solution are presented below:

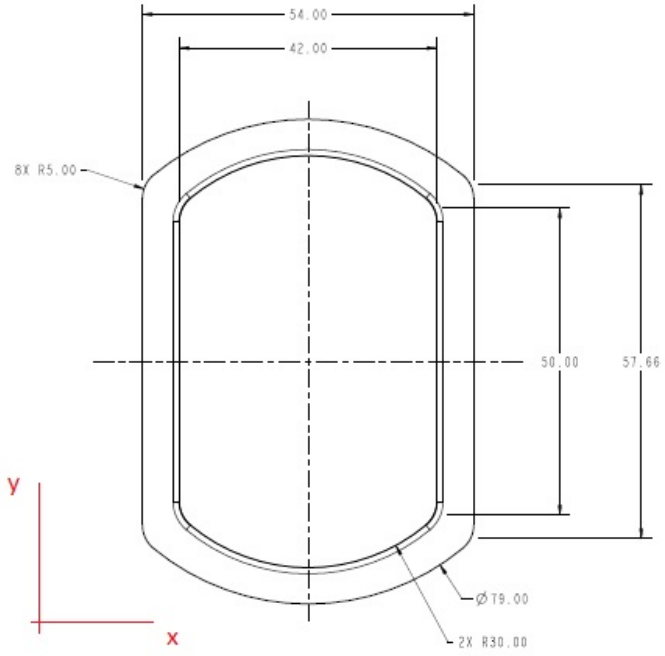

Figure 4.8: Glass window's original shape

This alteration in the window geometry implies changes in the other components, which are presented in the figures below. The front shell cavity was shaped in order to have the same geometry as the glass window. There were no other alterations.

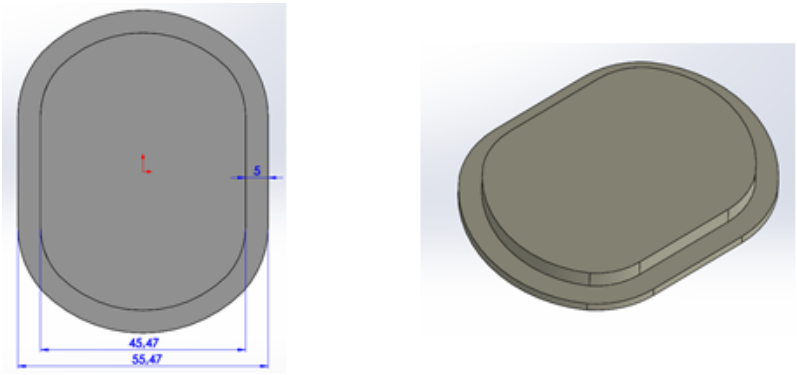

Figure 4.9: Glass window with rounded corners

The bezel suffered alterations but only on the side where it attaches to the glass (a), having the same geometry as the window so it could fit.

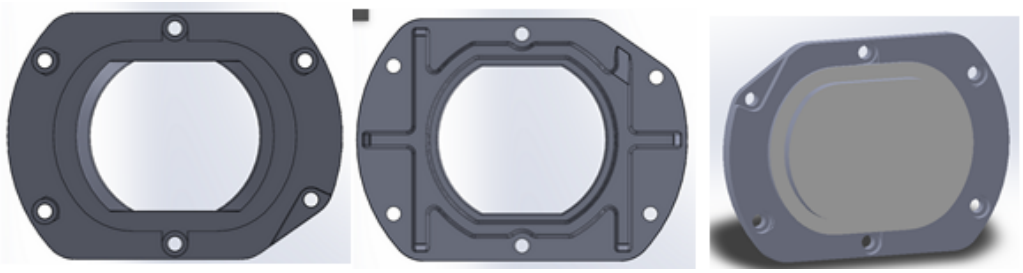

Figure 4.10: Bezel with a caviy with rounded corners for the glass window

The insulator was also shaped into the glass new geometry.

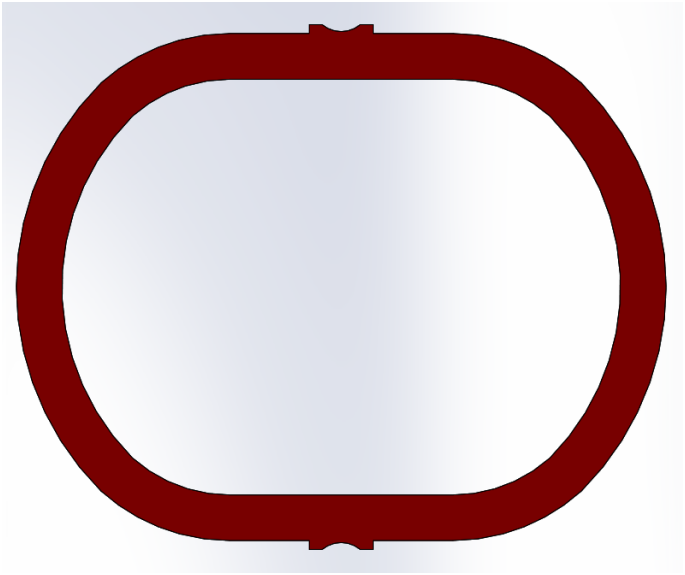

Figure 4.11: Insulator with rounded corners

Regarding the gasket, the strategy was slightly different, since its geometry was changed in order to follow the glass window geometry, but the transversal section was also modified, since a near-3-cylinder section seemed too rigid, and consequently a near-2-cylinder section was designed and tested.

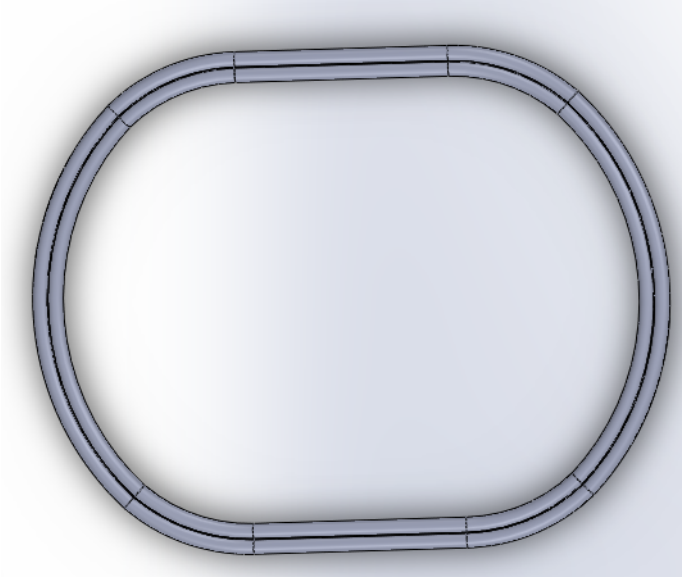

Figure 4.12: Gasket with rounded corners

The assembly of the components is presented in the following scheme:

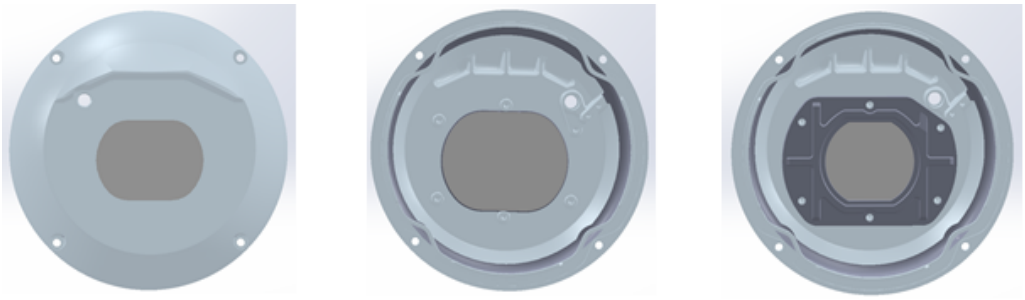

Figure 4.13: Assembly of the components with rounded corners

4.2 Plastics

Although the first approach to this issue is associated with the replacement of the SLS glass with other types of glass, there are polymeric materials which will also be considered, owing to their reduced brittleness and their ultimate strength. Besides, the most relevant requirements are transparency, clarity and scratch and impact resistance and therefore the proposed plastic materials here discussed are polycarbonate and acrylic.

4.2.1 Polycarbonate

Bosch had already developed a glass window prototype made of polycarbonate but because of the risk of yellowness throughout time, the company has decided to invest in a glass solution. Nonetheless, since this material presents some potential regarding the replacement of the glass window, owing to the good mechanical properties, it will still be analyzed and compared.

Polycarbonates belong to the thermoplastic group of polymers and are known for their strength, toughness and optically transparency, presenting high impact resistance, but low

scratch resistance. A polycarbonate has a larger plastic domain, since it can undergo large plastic deformation without breaking or cracking. Besides, it presents very good electrical insulation properties and high durability [39]. On the other hand, the main disadvantages are related to special care required while processing, pale yellow color, limited resistance to chemicals and ultra-violet light. Its applications include compact discs, automotive headlamp lenses, drinking bottles, visors, medical applications, and due to its good light transmission and protection against the UV, it is indicated for the production of rails, seat parts or lenses.

4.2.2 Acrylic

Polymethylmethacrylate (PMMA), commonly referred to as acrylic, is a transparent thermoplastic which is often preferred to polycarbonate due to its moderate properties, easy handling and processing and low cost. Besides, it also stands out from other polymers owing to its high light transmission, long service life and high resistance to UV light. In addition, PMMA presents the highest surface hardness among all the polymers and it is 100% recyclable.

4.2.3 Polycarbonate vs Acrylic

The comparison between these two materials leads to the following conclusions:

Polycarbonate

- Higher impact resistance;
- Lower scratch resistance;
- More expensive;
- More bendable under environment temperature (0-20°C);
- Poorer clarity; diffuses light.

Acrylic

- Lower impact resistance;
- More resistant to evenly distributed loads;
- Higher scratch resistance
- Does not yellow over time;
- Better clarity [40].

A comparison of the mechanical properties of both the thermoplastics and of soda lime glass is presented in table 4.2:

Table 4.2: Comparison between the mechanical properties of both polymers and SLS [40]

Property/Material	Polycarbonate	Acrylic	SLS
Density (kg/m^3)	1200-1400	1200	2530
Young Modulus (GPa)	13.5 - 21.4	3.2	72
Poisson's ratio	0.32	0.35-0.4	0.23
Tensile Strength - Ultimate (MPa)	66-160	71	41-180
Impact Strength (J/m)	140-440	74	
Thermal Expansion (m/mK)	10-69	76	8.8 - 9
Optical light transmission	89	92	89-90

Regarding the comparison between the two polymers, acrylic has a higher scratch resistance and better clarity while polycarbonate presents a higher impact strength but low scratch resistance. Acrylic will yellow more slowly over time and has an excellent light transmission capability and on the other hand polycarbonate is easier to work with since acrylic cannot shatter [40].

If a polycarbonate is chosen in order to replace the glass window, it is necessary to improve its properties by the implementation of a protective coating, such as a UV coating, since the UV attacks the outer surface and consequently the physical and chemical properties are affected, causing it to turn yellow. The coating's warranty will depend on the nature of the protective layer since although it can remain intact for a long period of time, eventually it will probably start to develop microcraks which can compromise its efficiency [41].

Besides, a hard coating would also be necessary since even though polycarbonate can withstand high magnitude of impact, it is not resistant to abrasion and this type of coatings ensure very good light clarity which improves transmission of light and resistance to chemical attack [41]. Based on the analysis of both materials, it is possible to conclude both present desirable and undesirable properties.

Acrylic will not turn yellow so easily, if it loses clarity it can be polished to regain it [42], presents better clarity and has higher scratch resistance. However, its shatter resistance is significantly lower which would lead to choose polycarbonate, but only with a protective and a hard coating.

Chapter 5

Results analysis

The numerical modulation was accomplished using the tridimensional models provided by Bosch and modified in the previous chapter. A mesh of tetrahedrons (with 49 936 elements for he first solutions, 53 115 for the second one and 61 436 for the third one) was generated and the purple face presented in figure 1 was considered as the fixed support in all the simulations. An applied stress of 5 bar ($\sim$ 500000 Pa) was chosen in order to simulate the watertighness test which takes place in the production line.

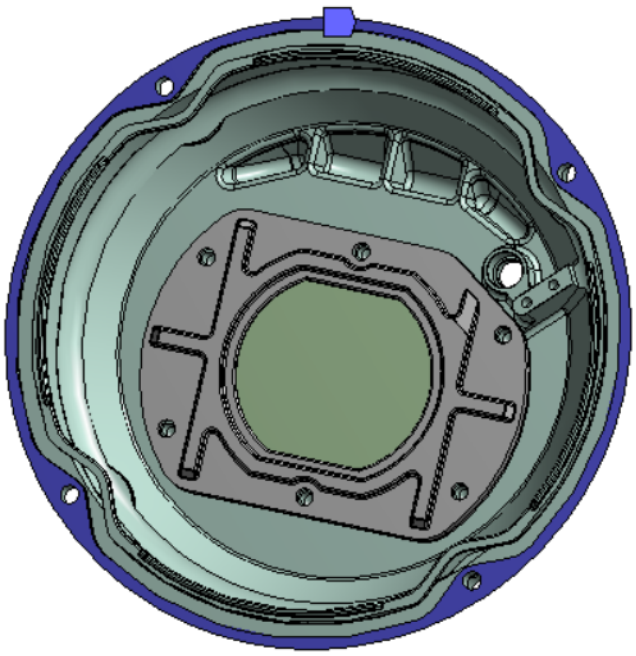

Figure 5.1: Purple: fixed support surface

Since the properties of some components were not provided, in order to carry out the simulation, the gasket and the insulator were considered to be made of polyurethane. Regarding the other components, the properties used in the numerical simulation are the ones considered in the Issue chapter.

The first step to consider when the simulation took place was to facilitate the process and therefore to reduce the number of faces of the front shell. In order to do so, the fins present in this component were removed, represented in figure 2.

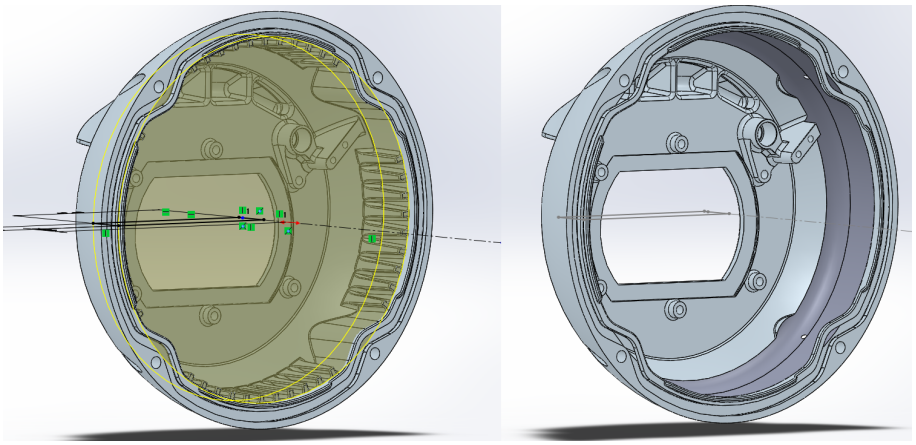

Figure 5.2: Removal of fins

The values of the equivalent stress obtained for the analyzed components will be compared with the yield strength of the corresponding materials:

- 41 - 80 MPa for the soda lime glass, before strengthening, which means a glass window would have a yield strength of 500 MPa (corresponding to the compressive stress rsultant from the stengthening) plus 41 MPa, in the worst case;
- 88 MPa for the aluminum alloy, although it might reach 165 MPa, considering a pressure die.

5.1 Results

5.1.1 Initial geometry

The results for the initial geometry for the glass window of MIC 7000 are presented in figure 5.3 and 5.4, regarding the stress and deformation fields, also considering a pressure of 5 bar and the the same surface as the fixed support.

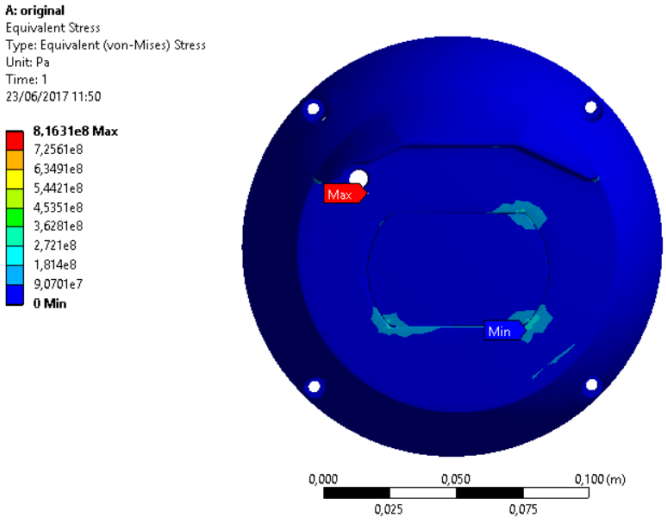

Figure 5.3: Equivalent stress for the initial geometry of the glass window considering the assembly

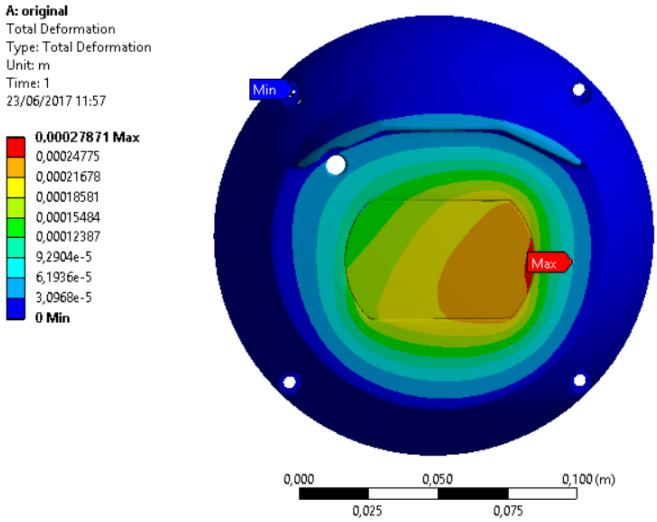

Figure 5.4: Deformation for the initial geometry of the glass window considering the assembly

Considering only the glass window, the results for the equivalent stress and deformation are shown in figure 5.5 and 5.6:

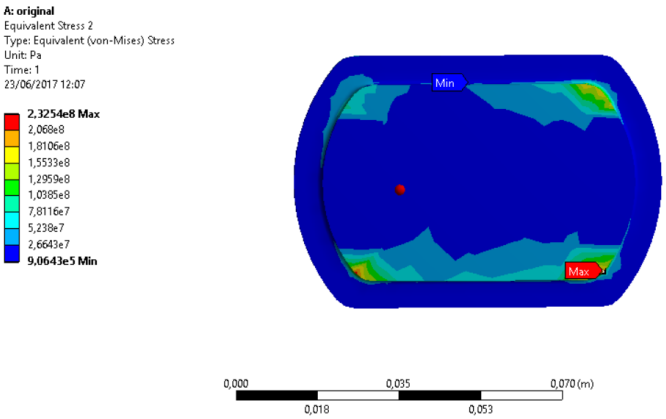

Figure 5.5: Equivalent stress for the initial geometry of the glass window

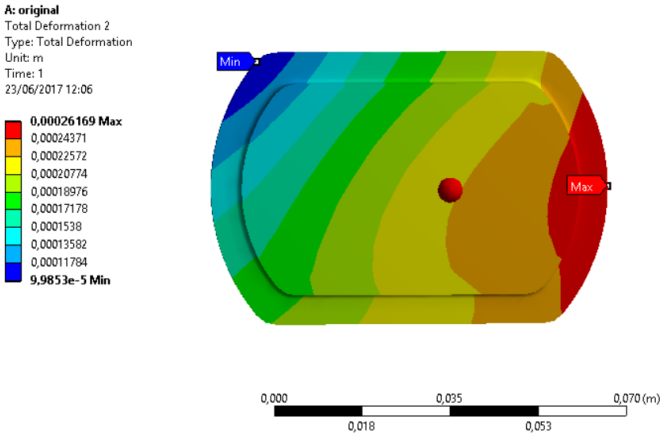

Figure 5.6: Deformation for the initial geometry of the glass window

It is possible to verify in figures 5.4 and 5.6 the maximum deformation area is located in the fourth corner which confirms the results provided by the ESPI method. Besides, in figure 5.5 where the equivalent stress for the glass window are presented, the corners exhibit once again the stress concentration areas, with a maximum of 233 MPa situated in the fourth corner.

5.1.2 Circular shape

The circular shape of the glass window and all the other components implies a non-uniform distribution of the deformation since the maximum deformation area is not located exactly in the center of the glass window but on the right side of it, which could lead to torsion, and consequently breakage, as it is presented in figure 5.7.

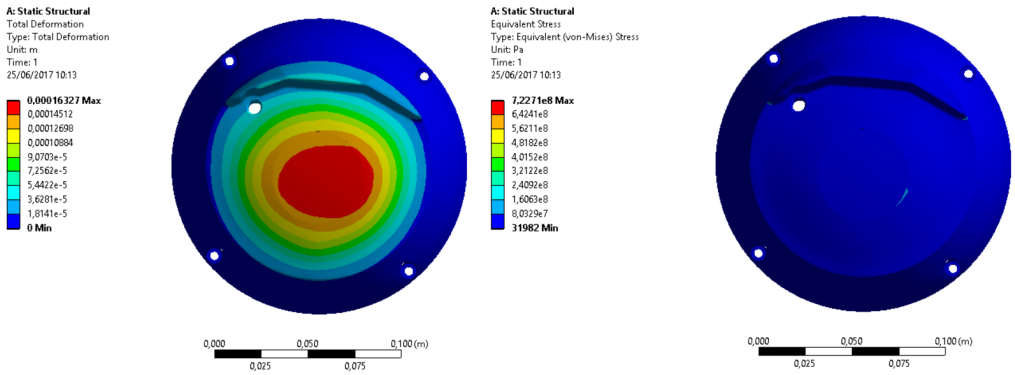

Figure 5.7: Deformation and stress of the assembly for a pressure of 5 bar

The maximum deformation for the glass window is 1.36×10^{-4} mm as well as for the entire assembly, while the maximum equivalent stress is 42 MPa in the glass and 100 MPa for the front shell, as it is presented in figure 5.8.

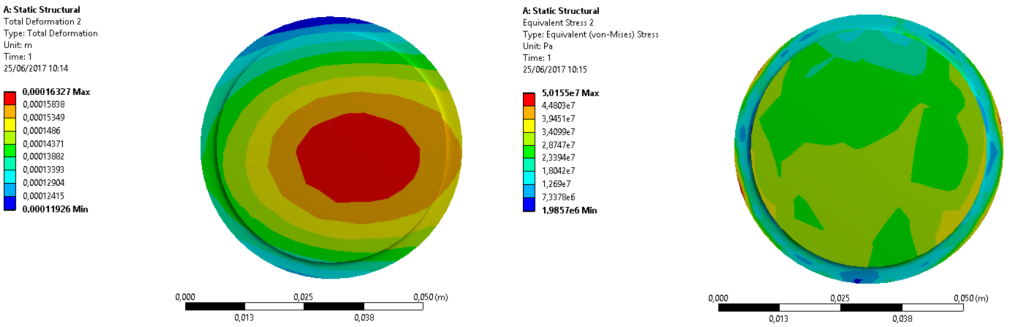

Figure 5.8: Deformation and stress of the glass window for a pressure of 5 bar

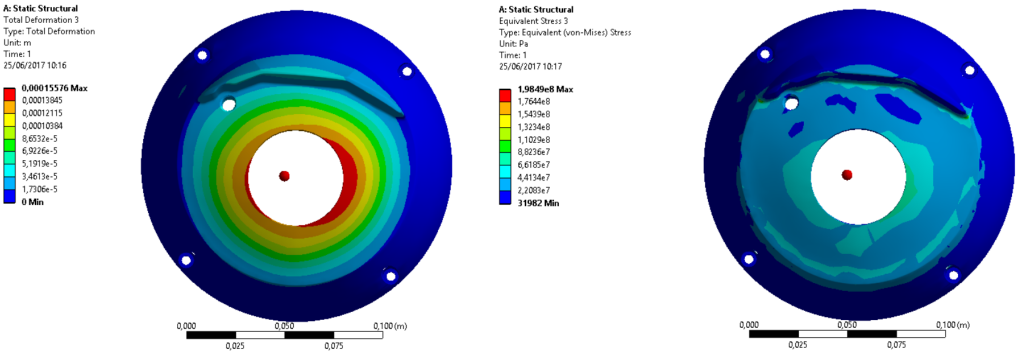

Figure 5.9: Deformation and stress of the front shell for a pressure of 5 bar

5.1.3 Circular shape with rib

The absence of symmetry in the results of a solution where a circular shape is considered has led to the introduction of a rib which could possibly compensate the presence of the rib for the wiper engine.

Considering figure 5.10, it is possible to verify the maximum deformation area is more uniform than the previous, although still non-symmetrical.

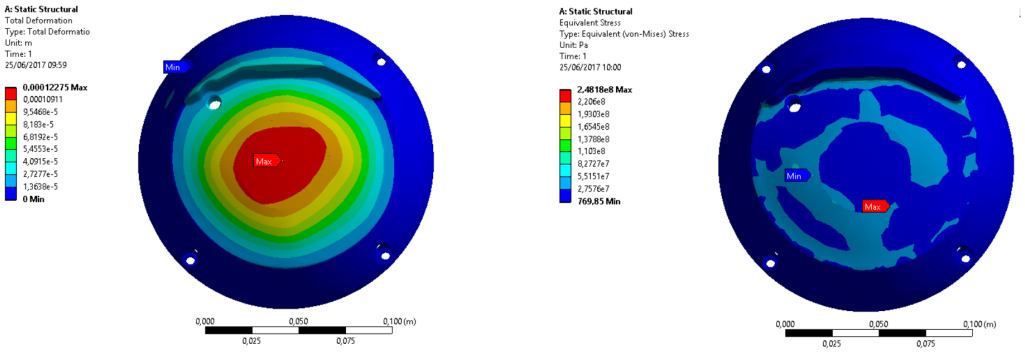

Figure 5.10: Deformation and stress of the assembly for a pressure of 5 bar

The maximum deformation for both the shell and the glass window is 1.23× 10^{-4} mm, and the maximum equivalent stress is 40 MPa for the glass window and around 100 MPa for the front shell.

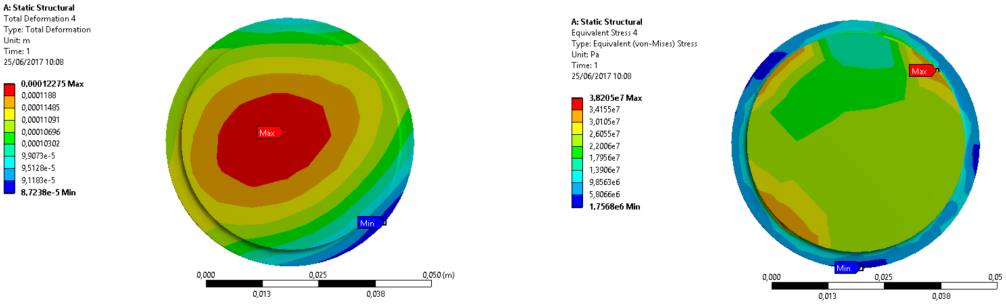

Figure 5.11: Deformation and stress of the glass window for a pressure of 5 bar

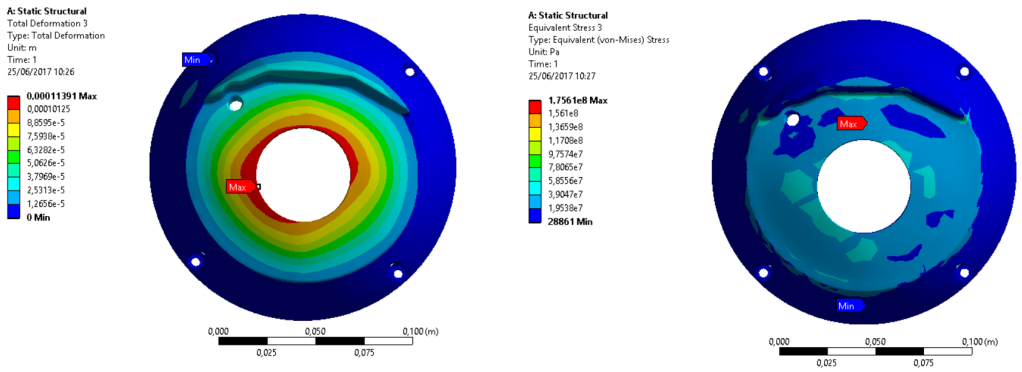

Figure 5.12: Deformation and stress of the front shell for a pressure of 5 bar

5.1.4 Rounded corners

The deformation distribuition of the assembly whose components present rounded corners is the most uniform of the three solutions, as it can be verified in figure 5.13. In figure 5.14 it is also possible to observe the maximum deformation area located exactly in the center of the window, leading to the desired symmetry.

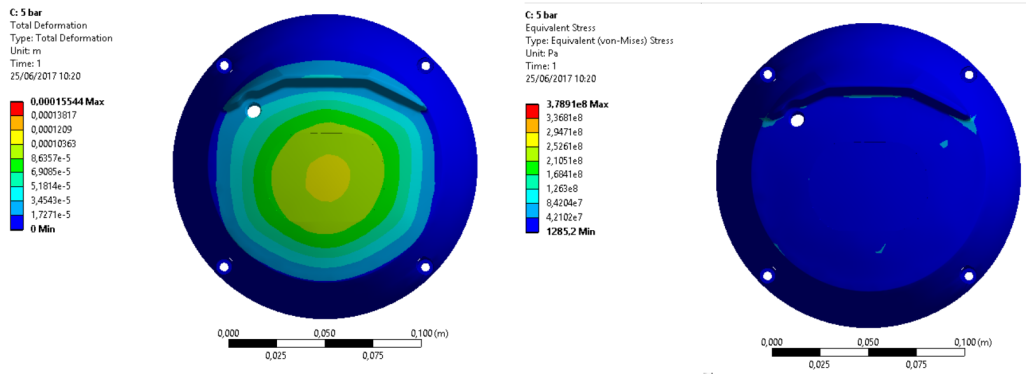

Figure 5.13: Deformation and stress of the assembly for a pressure of 5 bar

The maximum value of deformation for the front shell and for the glass window is around 1.55×10^{-4} mm while the maximum equivalent stress is 70 MPa for the glass window and 122 MPa for the front shell.

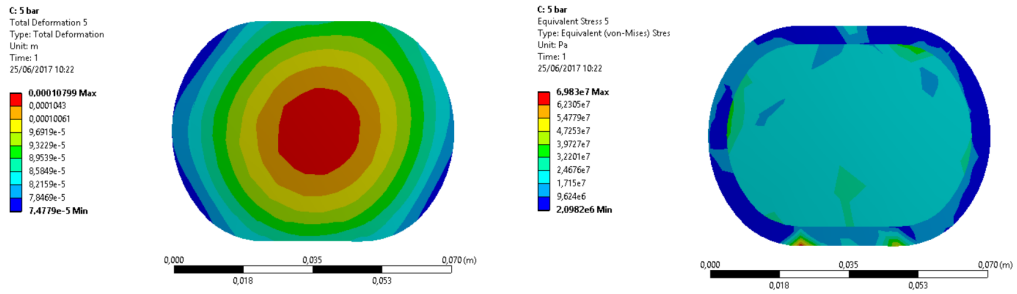

Figure 5.14: Deformation and stress of the glass window for a pressure of 5 bar

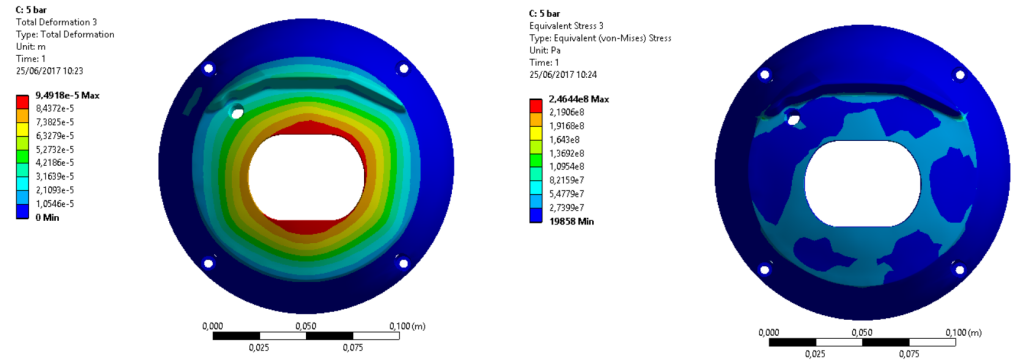

Figure 5.15: Deformation and stress of the front shell for a pressure of 5 bar

5.2 Conclusions

The two first solutions which consist of circular shapes do not present a uniform deformation field, since in the first case the maximum deformation is slightly offset to the right while on the second case it is on the left. However the solution which presents a glass window with rounded corners exhibits a deformation field with very uniform distribution since

it maximum is located exactly in the center of the glass window, ensuring this component will not twist. Besides, the stress concentration area associated to the corners present in the original solution, in figure 5.5, was eliminated.

With regard to the equivalent stress field, the values for this parameter obtained through the finite elements method are lower than the yield strength, considering all the solutions, which means the glass window will not break and the front shell will not reach the plastic domain.

It is of major importance to note the changes simulated above do not only concert the geometry of the glass window and the other components but also the gasket's cross section, from a near-3-cylinder to a near-2-cylinder. The figures of the components which present the stress field exhibit maximum values which do not actually correspond to the maximum stress they are subjected to. These values are due to geometry imperfections and interferences and do not affect the analysis of the numerical simulation.

Chapter 6

Conclusion

6.1 Conclusions

There is not a single reason to justify the glass window breakage since there is not a mechanism or a component which is contributing for failure. Instead there is a set of factors which combined together conduct to fracture.

The absence of dimensional tolerances is one of the main aspects which can possibly contribute to breakage. According to Bosch's internal report carried out by the processes department, there should more tolerances since its nonexistence can possibly contribute to the aggravation of the residual stress when the tightening torque is applied. The presence of impurities is also a matter of interest, since Bosch should ensure the components are free of dirt and in order to prevent the presence of it, the components should be clean before the assembly in the line.

The difference of the tightening torque found in the investigation carried out by INEGI, as well as the deviation present in the flatness measurement of the machined surface of the front shell and the residual stress concentration observed through the polariscope are factors which should be re-analyzed and rectified. The residual stress concentration was the first indicator of some imperfections regarding the chemical strengthening which added to an investigation considering the type of glass and the type of treatment led to some suspicions about the efficiency of this process. A study on the glass's surface which took place in CEMUP revealed the case depth resultant from strengthening was out of specification and therefore the increase of strength of this component was compromised. Besides, the SLS glass could be replaced for an alkali-aluminosilicate, a lithium-aluminosilicate, best suited for a chemical strengthening, or even for a polycarbonate with a hard and a protective coating.

The ESPI method presented a difference in the deformation of the front shell and the glass window, which will not be able to be rectified since the two components are made of materials with very different mechanical properties. In addition, the asymmetry of the front shell due to the rib of the motor engine leads the glass window not only to bend but also to twist. The first attempt to eliminate it was a circular shape, where later a rib was added in order to compensate the rigidity provided by the motor engine rib. Nonetheless, the results did not present the desired symmetry since the maximum deformation was not located in the center of the glass window.

The presence of the corners in the glass window geometry was seen as a contributor to failure and thus the geometry of this component was modified so these features could be eliminated. Three suggestions were made which led to conclude a glass window with rounded corners should be the best proposed solution, since it would not be very different

from the initial geometry, and consequently it would not compromise the 'brand geometry' of Bosch. Besides the results from the numerical simulation revealed the stress and deformation obtained woud ensure the window glass would not break.

6.2 Future Work

The gasket used for MIC 7000, due to its geometry, probably provides too much rigidity contributing to failure and therefore the development of less rigid gaskets, for instance with a different geometry, could be accomplished in order to be test so the water tightness ensured and to verify if it would affect the deformation field. The geometry of the gasket's cross section is also a matter of interest since it would be helpful to analyze the impact of different geometries, including the one proposed, in the watertightness test.

Acrylic and polycarbonate with coatings glass window prototypes could be develop since they consist of lightweight solutions with significant advantages when compared to glass.

Besides, a deeper analysis of the dimensional tolerances could also play an important role in improving the reduction the residual stress concentration after the tightening torque is attained, as well as the introduction of more relevant tolerances.

References

[1] F. Veer, "The strength of glass, a nontransparent value," *HERON-ENGLISH EDITION-*, vol. 52, no. 1/2, p. 87, 2007.

[2] R. Gy, "Ion exchange for glass strengthening," *Materials Science and Engineering: B*, vol. 149, no. 2, pp. 159–165, 2008.

[3] A. K. Varshneya, "Chemically strengthened lithium aluminosilicate glass having high strength effective to resist fracture upon flexing," Nov. 6 2012, uS Patent 8,304,078.

[4] N. Perez, "Introduction to fracture mechanics," in *Fracture Mechanics*. Springer, 2017, pp. 53–77.

[5] Bosch, "Bosch in portugal," http://www.bosch.pt, 2017-02-09.

[6] J. E. Shelby, *Introduction to glass science and technology*. Royal Society of Chemistry, 2005.

[7] I. Salvado, "General features about glasses," *Overall Aspects of Non-Traditional Glasses: Synthesis, Properties and Applications*, p. 3, 2016.

[8] C. G. Trade, "Our products," http://cyberglasstrade.com/product.html, 2017-06-21.

[9] G. A. Rosales-Sosa, A. Masuno, Y. Higo, and H. Inoue, "Crack-resistant al2o3–sio2 glasses," *Scientific reports*, vol. 6, 2016.

[10] J. Mecholsky, "Mechanical properties of glass: Lecture 12," Virtual Course on Glass - The Properties of Glass.

[11] A. K. Varshneya, "Chemical strengthening of glass: lessons learned and yet to be learned," *International Journal of Applied Glass Science*, vol. 1, no. 2, pp. 131–142, 2010.

[12] G. D. Quinn, "A history of the fractography of brittle materials," in *Key Engineering Materials*, vol. 409. Trans Tech Publ, 2009, pp. 1–16.

[13] A. K. Varshneya, *Fundamentals of inorganic glasses*. Elsevier, 2013.

[14] C. H. Wang, *Introduction to fracture mechanics*. DSTO Aeronautical and Maritime Research Laboratory Melbourne, Australia, 1996.

[15] R. Smith, "An introduction to fracture mechanics for engineers: Part i: Stresses due to notches and cracks," *International Journal of Materials in Engineering Applications*, vol. 1, no. 2, pp. 121–128, 1978.

[16] D. o. G. Owoeye, Seun; The Federal polytechnic and Ceramic, "Effects of temperature and time of ion-exchange on the mechanical behavior of chemically toughened soda-lime glass," *Songklanakarin Journal of Science and Technology*, p. 15, 2016.

[17] H. Morozumi, H. Nakano, S. Yoshida, and J. Matsuoka, "Crack initiation tendency of chemically strengthened glasses," *International Journal of Applied Glass Science*, vol. 6, no. 1, pp. 64–71, 2015.

[18] B. Caddy, *Forensic examination of glass and paint: Analysis and interpretation.* CRC Press, 2002.

[19] A. J. Burggraaf, *The mechanical strength of alkali-aluminosilicate glasses after ion exchange.* Philips' Gloeilampenfabrieken, 1966.

[20] Dinorex, "Dinorex - glass for chemical strengthening," http://www.neg.co.jp/en/product/dp/dinorex, 2017-02-15.

[21] H. Wang, G. Xing, X. Wang, L. Zhang, L. Zhang, and S. Li, "Chemically strengthened protection glasses for the applications of space solar cells," *AIP Advances*, vol. 4, no. 4, p. 047133, 2014.

[22] I. Donald and M. Hill, "Preparation and mechanical behaviour of some chemically strengthened lithium magnesium alumino-silicate glasses," *Journal of materials science*, vol. 23, no. 8, pp. 2797–2809, 1988.

[23] A. K. Varshneya, "The physics of chemical strengthening of glass: room for a new view," *Journal of Non-Crystalline Solids*, vol. 356, no. 44, pp. 2289–2294, 2010.

[24] M. A. Berthaume, "Food mechanical properties and dietary ecology," *American journal of physical anthropology*, vol. 159, no. S61, pp. 79–104, 2016.

[25] F. A. Tulleners, J. Thornton, D. Crim, and A. C. Baca, *Determination of Unique Fracture Patterns in Glass and Glassy Polymers.* University of California-Davis, Forensic Science Graduate Program, 2013.

[26] T. Ono and R. Allaire, "Fracture analysis, a basic tool to solve breakage issues," *Taiwan FPD Expo 2000*, 2000.

[27] U. of Cambridge, "Fracture surfaces," https://www.doitpoms.ac.uk/tlplib/BD5/fracture.php, 2017-03-08.

[28] Unknown, "Fracture mechanics," Glass Strength Strengthening: Lecture 13.

[29] R. C. Bradt, "The fractography and crack patterns of broken glass," *Journal of failure analysis and prevention*, vol. 11, no. 2, pp. 79–96, 2011.

[30] "Glass soil evidence," http://lorpub.gadoe.org/State

[31] K. A. Bitgue, "Glass," https://www.slideshare.net/iamkaripotter/glass-analysis.

[32] "Fractures," http://www.tpub.com/maa/190.htm.

[33] D. Peterson, "Hearts may be made of glass but so are windows," https://deathbetweenthecovers.wordpress.com/2013/04/04/hearts-may-be-made-of-glass-but-so-are-windows/.

[34] Dynacast, "Cold chamber die casting," https://www.dynacast.com/cold-chamber-die-casting, 2017-05-16.

[35] J. G. Kaufman and E. L. Rooy, *Aluminum alloy castings: properties, processes, and applications*. Asm International, 2004.

[36] C. P. Net, "Die casting," http://www.custompartnet.com/wu/die-casting, 2017-05-16.

[37] T. M. Gross, "Scratch damage in ion-exchanged alkali aluminosilicate glass: crack evolution and the dependence of lateral cracking threshold on contact geometry," *Fractography of advanced ceramics and glasses VI*, pp. 113–122, 2012.

[38] R. Tandon and S. J. Glass, "Controlling the fragmentation behavior of stressed glass," in *Fracture Mechanics of Ceramics*. Springer, 2005, pp. 77–91.

[39] P. Europe, "Polycarbonate (pc)," http://www.plasticseurope.org/what-is-plastic/types-of-plastics-11148/engineering-plastics/pc.aspx, 2017-05-31.

[40] Hydrosight, "Acrylic vs. polycarbonate: a quantitative and qualitative comparison," http://www.hydrosight.com/acrylic-vs-polycarbonate-a-quantitative-and-qualitative-comparison/, 2017-05-31.

[41] Excelite, "The essential polycarbonate protective coating for industrial applications," http://www.exceliteplas.com/the-essential-polycarbonate-protective-coating-for-industrial-applications, 2017-05-31.

[42] C. P. Sheeting, "Acrylic vs. polycarbonate," http://www.cutplasticsheeting.co.uk/blog/2013/11/29/acrylic-vs-polycarbonate/, 2017-05-31.

[43] M. Hill and I. Donald, "Stress profile characteristics and mechanical behaviour of chemically strengthened lithium magnesium aluminosilicate glasses," *Glass technology*, vol. 30, no. 4, pp. 123–127, 1989.

[44] A. K. Varshneya, "Chemical strengthening of glass: Lecture 27," Glass Processing.

[45] A. Taneja, "The extension of griffith's analysis," https://www.linkedin.com/pulse/extension-griffiths-analysis-ajay-taneja.

Appendix